https://doi.org/10.5194/egusphere-2026-2761
Preprint. Discussion started: 16 July 2026

A high-resolution coupled atmosphere-ocean model of the Great Barrier Reef: ACCESS-EMS-GBR v1.0

Rebecca L. Jackson[1], Matthew T. Woodhouse[2], Mark Baird[1], Clothilde Langlais[1], Mathieu Mongin[1], Anthony Jones[3,4], Daniel Partridge[4], Luke Harrison[5,6], Johanna Horchler[7,8], Joel Alroe[7], Luke Cravigan[7], Zoran Ristovski[7] and Daniel P. Harrison[6,9]

[1]CSIRO Environment, Hobart, 7004, Australia
[2]CSIRO Environment, Aspendale, 3195, Australia
[3]Met Office, Exeter, EX1 3PB, United Kingdom
[4]Department of Mathematics and Statistics, Faculty of Environment, Science and Economy, University of Exeter, Exeter, United Kingdom
[5]School of Aerospace, Mechanical and Mechatronic Engineering, University of Sydney, Sydney, 2006, Australia
[6]National Marine Science Centre, Southern Cross University, Coffs Harbour, 2450, Australia
[7]International Laboratory for Air Health and Quality, Queensland University of Technology, Brisbane, 4000, Australia
[8]Department of Chemistry, Faculty of Natural Science, Aarhus University, Aarhus, 8000, Denmark
[9]School of Geosciences, University of Sydney, Sydney, 2006, Australia

Correspondence to: Rebecca L. Jackson (rebecca.jackson@csiro.au)

Abstract. We present a new regional coupled atmosphere and ocean model of the Great Barrier Reef (GBR), Australia, called ACCESS-EMS-GBR. The model comprises a regional configuration of the Australian Community Climate and Earth System Simulator (ACCESS) atmospheric model (the United Kingdom Met Office Unified Model), coupled to the Commonwealth Scientific and Industrial Research Organisation Environmental Modelling Suite (EMS) hydrodynamic and biogeochemical model of the GBR. The model includes detailed aerosol and cloud microphysics in the atmosphere, as well as hydrodynamics, biogeochemistry, ecology and coral reef processes in the ocean. When coupled, the models form a valuable tool for simulating interactions between the atmosphere and ocean. The ACCESS-EMS-GBR model was developed to assess the plausibility and implications of marine cloud brightening (MCB) in the GBR, as part of the Reef Restoration and Adaptation Program (RRAP) Cooling and Shading Sub-program (RRAP-CS) but can also be utilised to study various processes including sources of marine aerosol and the impact of aerosol deposition on marine biogeochemistry. Here, we describe the model as configured for the GBR region, including the coupling framework, and evaluate the model skill in simulating measured aerosol and seawater temperature and irradiance. We configure the model aerosol scheme and emission sources to capture observed aerosol properties over the GBR region, with boundary layer nucleation and terrestrial biogenic emissions having a large influence on aerosol number concentration, size distribution and composition. The distribution of sea salt emissions is also expanded to include the soluble Aitken mode; a significant improvement in capability for simulating MCB and possibly for improving global climate model biases.

https://doi.org/10.5194/egusphere-2026-2761
Preprint. Discussion started: 16 July 2026

1 Introduction

Regional models are useful tools for studying spatially complex environments and to account for processes that are not resolved by global models (Giorgi, 2019). Coral reefs in particular require high-resolution modelling to capture regionally important features such as the coral reef matrix and processes including emissions of aerosol precursors (Deschaseaux et al., 2022; Swan et al., 2017), phytoplankton dynamics, nutrient cycling (Skerratt et al., 2019) and coral bleaching (Baird et al., 2018; Ellis et al., 2025).

As the frequency of coral bleaching events continues to rise, high-resolution models are increasingly needed to predict impacts and to help inform management practices (Melbourne-Thomas et al., 2011; Suggett & Smith, 2020). The Great Barrier Reef (GBR), Australia, has experienced eight mass thermal coral bleaching events since 1998, six of which have occurred since 2016. It is estimated that more than 98% of coral reefs in the GBR have been affected by bleaching during these events (Hughes et al., 2021), with adverse impacts on coral growth and calcification (De'ath et al., 2009; Razak et al., 2020), larval supply and stock-recruitment (Cheung et al., 2021; Hughes et al., 2019) leading to biodiversity loss and potential ecosystem collapse in future (Pratchett et al., 2021).

The Reef Restoration and Adaptation Program Cooling and Shading Sub-program (RRAP-CS) is researching and developing a range of interventions to help the GBR recover and adapt to the impacts of climate change. Regional marine cloud brightening (MCB) has been suggested as one way to mitigate coral bleaching in the GBR by reducing surface irradiance and temperature during summer (Harrison et al., 2019). The concept of MCB was first suggested by Latham (1990, 2004) and involves emitting sea spray aerosol from the sea surface into the lower atmosphere to enhance aerosol direct and first indirect effects (Twomey, 1974), thereby shading and cooling the sea below (Harrison, 2024; Harrison et al., 2019; Tagliafico et al., 2022). Given the predicted rise in global mean temperature, even under optimistic emission scenarios (IPCC, 2023), such interventions may be necessary to protect vulnerable ecosystems such as the GBR (Condie, 2022; Kleypas et al., 2021; Kwiatkowski et al., 2015).

Interventions such as MCB require thorough assessments to be undertaken to understand their efficacy, impacts and any unintended or undesirable consequences (McDonald et al., 2019). While numerous regional atmospheric and ocean models are available, the complexity of the MCB intervention requires a specialised and optimised regional coupled model, with detailed representation of aerosol and cloud microphysics in the atmosphere, as well as the physical and biological properties of the marine environment.

ACCESS-EMS-GBR is a high-resolution, regional coupled atmosphere-ocean model of the GBR and provides a valuable tool to undertake these assessments, being the first regional model capable of simulating the impact of aerosol emissions (including sea spray emissions for MCB) on clouds, radiation, precipitation and ecological responses to changes in temperature and light in the underlying coral reef. The model comprises a regional configuration of the Australian Community Climate and Earth System Simulator (ACCESS) atmospheric model (the United Kingdom Met Office Unified

https://doi.org/10.5194/egusphere-2026-2761
Preprint. Discussion started: 16 July 2026

Model) coupled to the Commonwealth Scientific and Industrial Research Organisation (CSIRO) Environmental Modelling Suite (EMS) hydrodynamic and biogeochemical model of the GBR. The model includes detailed aerosol and cloud microphysics in the atmosphere, as well as hydrodynamics, biogeochemistry, ecology and coral physiological processes in the marine environment, providing a valuable tool for ocean-atmosphere studies.

ACCESS is a suite of modelling tools used by the Australian community to simulate past, present and future climate and weather from global to local scales. EMS is a suite of ocean modelling tools developed by the CSIRO to simulate hydrodynamic and biogeochemical processes at the regional scale, with nesting capability. The EMS GBR configuration used here has a curvilinear horizontal grid spacing of approximately 4 km (henceforth GBR4) (Baird et al., 2020). The GBR4 configuration was developed for the eReefs project (Steven et al., 2019) and provides detailed information on the state of the marine environment to understand and address issues surrounding water quality, coral bleaching, ocean acidification, reef connectivity and to inform management processes. While developed for assessing MCB, the capabilities of the ACCESS-EMS-GBR model make it well suited for studying various other ocean and atmosphere processes in the GBR, such as sources of marine aerosol and precursors (Fiddes et al., 2022; Jackson et al., 2020), heat and radiation feedbacks (McGowan et al., 2022), links between meteorology and hydrodynamics during coral bleaching events (Richards et al., 2024, 2026), and biogeochemical cycles (Skerratt et al., 2019).

Both the regional ACCESS and EMS source models are relocatable and domains may be customised to regions of interest. Here, we describe and evaluate the ACCESS-EMS-GBR model as configured for the GBR region. Details of the coupling approach and parameters are provided, and possible applications and areas for future development of the coupled model are discussed. The model skill in capturing observed aerosol, seawater temperature and irradiance in the GBR are evaluated against observations from recent RRAP-CS field campaigns and in-situ monitoring networks. Details of the approach to simulate MCB and the impact on cloud, radiation, precipitation and ecological processes in the coral reef, along with a detailed evaluation of cloud properties, will be presented in a follow-up paper.

2 Model setup

2.1 Atmospheric model

The atmospheric component of ACCESS-EMS-GBR is the United Kingdom Met Office Unified Model (UM, version 13.0). The UM Regional Nesting Suite (RNS) supports one-way nesting of limited area domains within the global UM or a reanalysis dataset. Here, the global UM is used as the driving model and provides initial and hourly boundary conditions to the regional atmospheric model.

The global model configuration is based on the Global Atmosphere 8 and Global Land 9.0 (GA8-GL9) science configuration (Willett et al., 2026) and is run on the 'N216' grid, which has a horizontal grid-spacing of approximately 65 km at the mid-latitudes and 70 vertical levels (surface-80 km). Simulated meteorology is constrained by nudging the global model to the

https://doi.org/10.5194/egusphere-2026-2761
Preprint. Discussion started: 16 July 2026

European Centre for Medium-Range Weather Forecasts Reanalysis version 5 (ERA5) dataset (Hersbach et al., 2020). Nudging of temperature and horizontal winds is applied above the boundary layer every three hours.

The nested domain covers north-eastern Australia, the GBR and part of the Coral Sea (referred to here as NE AUS; Fig. 1). The NE AUS domain has a horizontal grid-spacing of 0.04° (approximately 4 km) and 90 vertical levels (including 17 below 1 km), reaching a model top of 40 km. The atmospheric component of ACCESS-EMS-GBR is called 'ACCESS-GBR' and uses the Regional Atmosphere and Land version 3.2 (RAL3.2) science configuration (Bush et al., 2025). The nested domain may be free-running or re-initialised daily, depending on simulation requirements. However, meteorology will always be constrained to the global simulation at the domain boundary, preventing simulated meteorology deviating far from reality. Here, the nested domain is re-initialised daily using initial conditions from the nudged global model to enable a better comparison between simulated and measured variables. The aerosol fields are re-initialised from the end of the previous cycle to allow aerosol mass and number concentration to persist through time and thus, are always free-running. Each cycle has a 48-hour forecast period, with the second 24-hour period of simulation used in the analyses below. Land surface processes are represented by the Joint UK Land Environment Simulator (JULES) (Best et al., 2011; Clark et al., 2011).

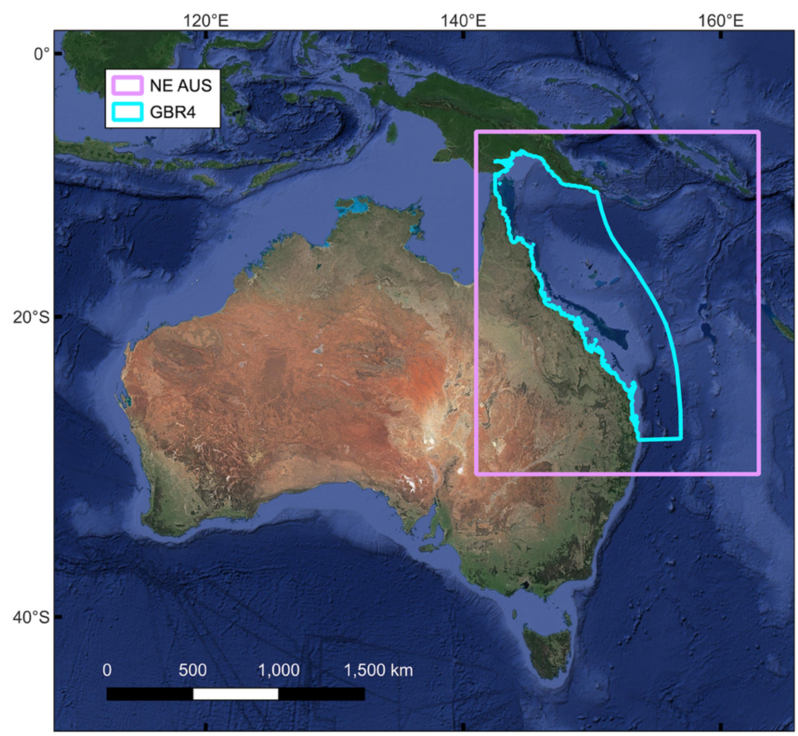

Figure 1. Map of Australia showing the regional atmosphere domain over north-eastern Australia (NE AUS; 0.04° horizontal grid-spacing) and the regional ocean domain (GBR4; approximately 4 km horizontal grid-spacing on a curvilinear grid). Basemap image © 2026 Google Satellite.

https://doi.org/10.5194/egusphere-2026-2761
Preprint. Discussion started: 16 July 2026

2.1.1 Aerosol and atmospheric chemistry

In both the global and regional domains, atmospheric composition is simulated by the United Kingdom Chemistry and Aerosol (UKCA) model. Aerosol processes are represented by the GLObal Model of Aerosol Processes modal version (GLOMAP-mode) aerosol scheme (Mann et al., 2012; Mann et al., 2010). GLOMAP-mode is a double-moment scheme (mass and number concentration) that represents the full aerosol cycle from emission through to deposition. The aerosol size distribution is simulated in five log-normal size modes (four soluble modes: nucleation, Aitken, accumulation and coarse; and one insoluble Aitken mode), with sulphate (from primary and secondary sources), sea salt, organic carbon (representing organic matter from primary and secondary sources, with a ratio of organic matter:organic carbon of 1.4) and black carbon aerosol species represented within each mode. The mean dry particle diameter, geometric standard deviation and aerosol species contributing to each size mode is shown in Table 1. Dust is represented separately as per Woodward (2001).

Table 1. Aerosol size modes and chemical species represented in ACCESS-GBR.

Mode	Dry diameter (nm)	Geometric standard deviation	Species[1]
Soluble nucleation	< 5	1.59	SO_4, OC
Soluble Aitken	5 – 50	1.59	SO_4, OC, BC, SS[2]
Soluble accumulation	50 – 500	1.40	SO_4, OC, BC, SS
Soluble coarse	> 500	2.00	SO_4, OC, BC, SS
Insoluble Aitken	5 – 50	1.59	OC, BC

[1]SO_4 = sulphate, OC = organic carbon, BC = black carbon, SS = sea salt. [2] Introduced in this work.

Emissions of natural aerosol (e.g. sea salt and primary marine organics) and precursor gases (e.g. dimethylsulfide, DMS) are calculated by the model using simulated wind speed and prescribed surface concentrations. Emissions of anthropogenic and terrestrial aerosol and precursors are prescribed. Prescribed oxidant concentrations are used to simulate the oxidation of aerosol precursors, including the oxidation of DMS to sulphur dioxide and further to sulfuric acid.

2.1.2 Revised aerosol setup

Initial ACCESS-EMS-GBR simulations strongly underestimated simulated aerosol number concentration (N10, dry diameter >10 nm) over the GBR (see Results). Conversely, the model captured the number concentration of cloud condensation nuclei (CCN) and aerosol composition reasonably well, indicating that the model was missing sources of smaller Aitken mode

https://doi.org/10.5194/egusphere-2026-2761
Preprint. Discussion started: 16 July 2026

aerosol. The below changes were made to address the bias in simulated aerosol. The extent to which these changes have reduced biases is discussed in the Results.

Firstly, the UM and UKCA source code was updated to allow sea salt to be emitted into the soluble Aitken mode (see Code Availability statement) (Table 1). Sea salt is an important source of aerosol over the GBR (Z. Chen et al., 2019; Eckert et al., 2024) and is typically emitted into the soluble accumulation and coarse modes in GLOMAP-mode. However, sea salt emissions are not emitted into the soluble Aitken mode in the standard configuration, potentially contributing to the underestimate of aerosol number concentration. The addition of Aitken mode sea salt has allowed emissions (both natural and for simulating MCB) to be more realistically distributed over the Aitken to coarse size modes, representing a significant improvement in capability, both for simulating MCB and possibly for reducing long-standing biases in climate models (Fiddes et al., 2025). The model currently simulates natural sea salt emissions using a wind speed-dependent parameterisation (Gong, 2003), which may be updated to include the influence of SST in future (Venugopal et al., 2025).

Prescribed anthropogenic surface-level emissions of sulphur dioxide and organic and black carbon from biofuel and fossil fuel sources (using the model emission assumptions for fossil fuel) were initially represented as a time-slice for the year 2014 derived from the Coupled Model Intercomparison Project Phase 6 (CMIP6). To reduce uncertainty associated with the anthropogenic emissions, the global and regional emissions were updated to use data from the Emissions Database for Global Atmospheric Research (EDGAR) Community Greenhouse Gas database (Crippa et al., 2024) for the year 2022. The sectoral assumptions of the emissions were also updated, with sulphur dioxide emitted at both the surface and lofted into the atmosphere (e.g. from ship stacks), and biofuel and fossil fuel emissions (and respective emission size assumptions) represented separately. At the global scale, the impact of the 2022 anthropogenic emissions is a decrease in the annual total anthropogenic sulphur dioxide (-265.5 Tg yr^{-1}), organic carbon (-11.4 Tg yr^{-1}) and black carbon (-9.4 Tg yr^{-1}) emissions. Over the NE AUS domain, the annual total anthropogenic sulphur dioxide emissions also decreased (-1.8 Tg yr^{-1}), yet the organic (0.06 Tg yr^{-1}) and black carbon (0.08 Tg yr^{-1}) emissions increased. The large reduction in sulphur dioxide emissions relative to organic and black carbon is largely due to the introduction of the International Maritime Organization 2020 regulations, which reduced the global limit on the sulphur content of shipping emissions from 3.5% to 0.5% (IMO, 2020).

Organics (from primary and secondary sources) are an important component of aerosol over the GBR (Horchler et al., 2025; Mallet et al., 2016). Primary marine organics are emitted in the model as primary marine organic carbon (PMOC), using assumptions for the modal mean dry diameter (160 nm), geometric standard deviation (2.0) and emission mode (25% / 75% to the soluble / insoluble Aitken mode), and at a rate that is dependent on wind speed, surface chlorophyll-*a* concentration and primary sea salt emissions (Gantt et al., 2012; Gantt et al., 2015). To better represent the PMOC component of sea spray aerosol across the soluble Aitken to coarse modes, and to help improve the Aitken mode low bias, we reduce the emission mean dry diameter from 160 nm to 40 nm.

Monoterpene emissions from terrestrial vegetation are another important source of organics, particularly over the Australian region (Emmerson et al., 2016). Monoterpenes are oxidised by hydroxyl, ozone and nitrate species in the model to form secondary aerosol precursors, which influence the rate of new particle formation in the lower atmosphere when boundary layer nucleation is enabled. Emissions were initially derived from biomass burning sources. However, the background terrestrial vegetation source is approximately two orders of magnitude larger over Australia and so monoterpene emissions were instead prescribed by a climatology (2001-2010) from the Model of Emissions of Gases and Aerosols from Nature - Monitoring Atmospheric Composition and Climate project (MEGAN-MACC) biogenic emission inventory (Sindelarova et al., 2014).

Lastly, organic-mediated boundary layer nucleation (BLN) was enabled in the model. The parameterisation of Metzger et al. (2010) is used, producing new particles (1.5 nm dry diameter) at a rate that is determined by the concentration of gas-phase sulfuric-acid and secondary organic aerosol (SOA). The SOA yield may be scaled to adjust the BLN rate in the model and from UM v12.0 is scaled to a factor of 0.13, which has been shown to substantially improve agreement with observed aerosol number concentrations in the lower atmosphere (Ranjithkumar et al., 2021). Here, the SOA yield is further scaled to a factor of 0.1 (0.013) in both the global and regional domains to adjust the BLN rate for the large source of monoterpene emissions and secondary organics over Australia. Doing so helped to reduce the modelled CCN bias, where CCN was occasionally overestimated, possibly due to condensational growth of the Aitken mode to the accumulation mode in the presence of high concentrations of condensable vapours from the oxidation of monoterpenes over the Australian region (see Results).

2.1.3 Large-scale cloud and precipitation

Large-scale cloud cover is represented by the Prognostic Cloud and Prognostic Condensate (PC2) scheme (Wilson et al., 2008). Convection is parameterised in the global model, with large-scale precipitation simulated via the auto-conversion of cloud droplet number concentration (from GLOMAP-mode) to rain droplets. In the nested domain, GLOMAP-mode is coupled to the Cloud AeroSol Interacting Microphysics (CASIM) cloud microphysics scheme (Field et al., 2023; Shipway & Hill, 2012). CASIM is a double-moment scheme that represents the mass and number concentration of five hydrometeor classes (cloud liquid water, rain, ice, snow and graupel). When coupled to GLOMAP-mode, simulated aerosol mass, size, number concentration, and composition are used to calculate cloud droplet number concentration, improving the representation of CCN activation to cloud droplets (Abdul-Razzak & Ghan, 2000) and surface precipitation at convection-permitting resolutions (Field et al., 2023). We also implement the recommendations of Ghosh et al. (2025), where the Abdul-Razzak and Ghan (2000) activation scheme is updated to improve simulated cloud droplet concentration and aerosol-cloud radiative effects (see Code Availability statement). These updates are expected to improve the representation of cloud droplet activation under very high CCN concentrations (such as can occur for MCB), where the non-monotonic Abdul-Razzak and Ghan (2000) scheme can unrealistically suppress activation (Tippett et al., 2026).

https://doi.org/10.5194/egusphere-2026-2761
Preprint. Discussion started: 16 July 2026

GLOMAP-mode and the cloud schemes are also coupled to the Suite of Community Radiative Transfer Codes based on Edwards and Slingo, 1996 (SOCRATES) radiation scheme to represent aerosol direct and indirect effects. Further details of the radiation scheme are provided in Bush et al. (2020).

2.2 Ocean model

The regional ocean circulation, biogeochemical properties and coral reef ecosystem are represented by the CSIRO EMS marine model of the GBR. The GBR4 (~4 km horizontal grid spacing on a curvilinear grid) configuration used here has 48 vertical levels with a model domain that covers the GBR and part of the Coral Sea (Fig. 1). A description of the GBR4 hydrodynamic and biogeochemical components is provided in Baird et al. (2020). ACCESS-EMS-GBR currently uses version 4.0 of the GBR4 hydrodynamics and version 4.2 of the GBR4 biogeochemistry, as described in Maggiorano et al. (2025), with modified atmospheric forcings.

In ACCESS-EMS-GBR, GBR4 is initialised using model output from the eReefs GBR4 hindcast archive (see Data Availability statement). The open ocean boundary conditions for seawater temperature, salinity, sea surface elevation and current velocities are provided by the Bluelink Reanalysis version 2020 (BRAN2020) (Chamberlain et al., 2021). Inputs from 64 rivers along the Queensland coastline are specified as open boundaries with inputs of momentum, freshwater, nutrients and sediment. An additional 37 sources of nutrients and sediments are also represented. The riverine inputs into the Great Barrier Reef Marine Park area are derived from the Dynamic SedNet catchment model (Ellis, 2018; McCloskey et al., 2021), while riverine inputs further south are derived from the Queensland Government Water Monitoring Network.

2.2.1 Hydrodynamics

The EMS Sparse Hydrodynamic Ocean Code (SHOC) (Herzfeld, 2006) represents hydrodynamic processes in the GBR4 model. SHOC simulates seawater temperature, salinity, density, current velocity, mixing coefficients, sea level and other physical states on a three-dimensional curvilinear grid.

The sea surface may fluctuate between vertical levels, as can the thickness of the upper-most layer to account for increases in sea surface elevation, such as can occur with thermal expansion or tidal variations. Tides are explicitly represented using amplitude and phase of the main eight constituents derived from the Topex Poseidon crossover solution 9.1 (TPXO9v1) ocean tide model (Egbert & Erofeeva, 2002). Simulating the depth of water over the coral reef allows the influence of tide on heating of shallow reef waters to be resolved (although this is best captured in higher resolution nested configurations), which is an important process for coral physiology (Buckee et al., 2020) and for emissions of aerosol precursors such as DMS (Hopkins et al., 2016; Swan et al., 2017).

The hydrodynamic and biogeochemical components are computationally demanding and operate across different time-steps, meaning that they are inefficient when fully coupled. To overcome this, SHOC is run in 'transport mode', where the system

https://doi.org/10.5194/egusphere-2026-2761
Preprint. Discussion started: 16 July 2026

is run in stages. The hydrodynamic model is run first on its native time-step (seconds) with outputs saved hourly. The hourly hydrodynamic outputs are then used in a flux form semi-Langragian (FSSL) advection scheme (Gillibrand & Herzfeld, 2016) to advect and diffuse biogeochemical and sediment tracers (with an hourly time-step). The FSSL advection scheme allows SHOC to be run with longer time steps (reducing computing time), while accurately reproducing tracer distribution and mass conversation (Herzfeld & Engwirda, 2023).

2.2.2 Biogeochemistry

The biogeochemical component of the GBR4 model consists of ecology, optical, carbon chemistry and sediment transport models, which together simulate the productivity, composition and optical properties of the water column and the benthic and sediment layers. Processes specific to coral reef ecosystems are also represented, including coral calcification, coral-algal symbiont dynamics and coral bleaching (Baird et al., 2018). A detailed description of the biogeochemical models is provided in Baird et al. (2020). A brief overview is provided below.

In the pelagic and epibenthic zones, the ecology model simulates the growth and mortality of plankton, seagrasses and corals. Four phytoplankton types (small and large phytoplankton, microphytobenthos and *Trichodesmium*) and three seagrasses (*Zostera*, *Halophila* and a general seagrass group) are represented. Benthic communities (e.g. corals and seagrasses) are represented as a biomass per square meter and influence water column nutrient concentration through growth, respiration and mortality. Phytoplankton and algal growth through photosynthesis is calculated from the amount of photosynthetically active radiation (PAR) and dissolved ammonium, nitrate, phosphate and inorganic carbon concentrations. Algae contain chlorophyll-*a* (chl-a) and accessory pigments, and carbon:pigment ratios that vary in response to light availability and photoadaptation.

Corals are represented as a total biomass of the coral host and zooxanthellae (photosynthetic endosymbionts). Zooxanthellae photosynthesis and growth is represented in the same way as for phytoplankton. Organic matter is assimilated by the coral host via both translocation from zooxanthellae and via the capture of detritus in the water column. A mechanistic coral bleaching process is included, which simulates the build-up of reactive oxygen species in zooxanthellae photosystems, coral oxidative stress and zooxanthellae expulsion based on the relationship between temperature, light and photosystem reaction centre dynamics (including photo-adaptation and inhibition). The coral bleaching scheme is described in detail in Baird et al. (2018) and calibrated using Ellis et al. (2025).

Gas exchange of oxygen and carbon dioxide (CO_2), cycling of nitrogen (N), phosphorus (P) and carbon (C), detritus remineralisation and the calcification and dissolution of carbonate structures (including corals) is represented. A carbon chemistry model represents the speciation of dissolved inorganic C along with the calculation of pH and carbonate saturation states.

https://doi.org/10.5194/egusphere-2026-2761
Preprint. Discussion started: 16 July 2026

Radiative transfer through the water column and other optical properties are forced using surface downwelling short-wave radiation (SWR). The GBR4 configuration used in ACCESS-EMS-GBR differs from that used in eReefs by using prescribed SWR from the atmospheric model (see Sect. 2.4.2) instead of calculating SWR as a function of solar zenith angle and cloud cover. Total surface downwelling SWR is provided to SHOC, which accounts for sea surface albedo, calculated as a function of solar zenith angle and wind speed (Zillman, 1972), with the latter also provided by the atmospheric model. The influence of atmospheric composition (aerosol and gaseous species) is accounted for in the prescribed total surface SWR, ensuring consistency in net surface SWR between the atmospheric and ocean models. Light attenuation through the water column is influenced by microalgae (including the concentration of photosynthetic pigments), detritus, dissolved organic matter and inorganic particles (e.g. suspended sediment), with self-shading also represented at the seabed for macroalgae, seagrasses and corals. Outgoing irradiance is influenced by the seabed colour, determined by benthic composition. Details of the inherent and apparent optical properties of each light attenuating component are provided in Maggiorano et al. (2025).

Inorganic and organic compounds are exchanged between the water column and sediment. A sediment transport model represents the sinking, deposition and resuspension of gravel, sand, mud and dust in various size classes. Sediment resuspension is influenced by simulated current velocity, wave amplitude period and orbital velocity through the computation of the bottom sheer stress at the seabed, based on the equations of Grant and Madsen (Grant & Madsen, 1982; Madsen, 1994). Waves are simulated by AUSWAVE (Australian Wave Model) (Zieger & Greenslade, 2021; Zieger, 2025), a spectral wave forecasting model adapted from the National Oceanic and Atmospheric Administration (NOAA) WAVEWATCH III model and operated by the Australian Bureau of Meteorology and CSIRO. Further detail on the sediment transport model are provided in Margvelashvili et al. (2009, 2018).

2.3 Coupling approach

The atmosphere NE AUS domain is coupled to the ocean GBR4 domain using a simple and customizable approach. The models run consecutively, exchanging respective atmospheric and ocean forcings at daily intervals. The tasks required to run the GBR4 model and post-process the model outputs (for compatibility) have been incorporated into the ACCESS-GBR workflow.

An option has been added to the ACCESS-GBR suite configuration to enable the atmosphere to run with GBR4 as the coupled ACCESS-EMS-GBR model. When enabled, the atmospheric and ocean models run consecutively, pausing and exchanging forcings each day. After each day of atmosphere simulation, atmospheric forcing files are created and used to force the GBR4 hydrodynamic and biogeochemical model for the same day. On completion of each GBR4 simulation, the sea surface forcings are updated with the GBR4 outputs and used to force the next day of atmosphere simulation.

The limitation of this approach is that the models must run consecutively. The atmosphere typically has a shorter circulation time and responds to changes in radiative forcing faster than the ocean. Thus, ACCESS-GBR was chosen to run ahead of GBR4. Consequently, the atmosphere is forced by the mean sea surface state from the previous day within the GBR4

https://doi.org/10.5194/egusphere-2026-2761
Preprint. Discussion started: 16 July 2026

domain. While using the previous day's sea surface conditions is a limitation, the coupling approach still allows feedbacks in surface heat and radiation fluxes to be captured at the sea surface at daily resolution and provides a good representation of variability in daily mean sea surface temperature (SST).

More advanced coupling approaches were considered however, the offline approach described here minimises developmental overhead, while enabling flexibility in the coupling parameters and simulation requirements. The pause-resume approach also reduces computational costs, as no cost in computing time is incurred when the atmospheric model is held while the ocean model completes each day of simulation (and vice versa). Currently, running ACCESS-EMS-GBR on the Australian National Computational Infrastructure (NCI) requires approximately 2.5 hours of walltime and 2.3 kSU per simulated day (inclusive of the 48-hour atmosphere forecast, 24-hour ocean simulation and processing tasks), where 1 SU is 0.5 compute hours.

2.4 Coupled fields

Coupled variables are chosen to capture key feedbacks between the atmosphere and ocean surface. A small number of variables are currently coupled, however, coupling of additional variables is possible and would be straightforward using the existing framework.

2.4.1 Coupled ocean fields

In the atmospheric model, sea surface fields are prescribed by monthly-varying ancillary files (Willett et al., 2026). In both ACCESS-GBR and ACCESS-EMS-GBR, SST is prescribed by a daily mean ancillary file and is used to calculate sea-air heat fluxes. The net surface heat fluxes are balanced in the models, as is demonstrated in Appendix A.

For consistency with the GBR4 model boundary conditions, SST is prescribed by a daily mean dataset, derived from the BRAN2020 near-global (approximately 75°N-75°S) reanalysis product (Chamberlain et al., 2021). The BRAN2020 SST data are available at 10 km horizontal grid-spacing and were regridded to the global N216 grid and NE AUS 0.04° grids using a bilinear interpolation (xESMF; Zhuang et al., 2025), with nearest source to destination extrapolation to ensure alignment of the land-sea masks. Global data beyond 75 degrees North and South were filled using the climatological SST from the Met Office Hadley Centre Sea Ice and Sea Surface Temperature (HadISST) monthly mean dataset (Rayner et al., 2003), used in some configurations of the ACCESS global model. While this approach would be problematic for nested domains beyond 75° latitude, our configuration is focused on north-eastern Australia, where prescribing the BRAN2020 SST provides benefits that justify its use (e.g. consistency with the ocean model and availability at daily frequency).

When run as the coupled model (ACCESS-EMS-GBR), the prescribed SST is updated with GBR4 daily mean SST as the simulation progresses. To smooth the transition between the BRAN2020 and GBR4 SST, a bilinear interpolation is applied

https://doi.org/10.5194/egusphere-2026-2761
Preprint. Discussion started: 16 July 2026

across 10 grid cells at the boundary of the two datasets. The resulting merged BRAN2020-GBR4 SST is then used to force the global and regional atmospheric domains in ACCESS-EMS-GBR.

The daily mean BRAN2020 ancillary data provides a good representation of SST over short time-scales of days to weeks, which is important for capturing the impacts of changes in light and temperature in the atmosphere. Elevated SST above the climatological average is also represented (and is important for the MCB application), as is illustrated in the example ancillary data for February 2022, which is more than 4°C above the climatological mean (from HadISST, Fig. 2A) during the lead up to the 2022 coral bleaching event in the GBR (Fig. 2B). The merged BRAN2020-GBR4 SST additionally captures the influence of surface currents and upwelling along the continental shelf (Fig. 2C).

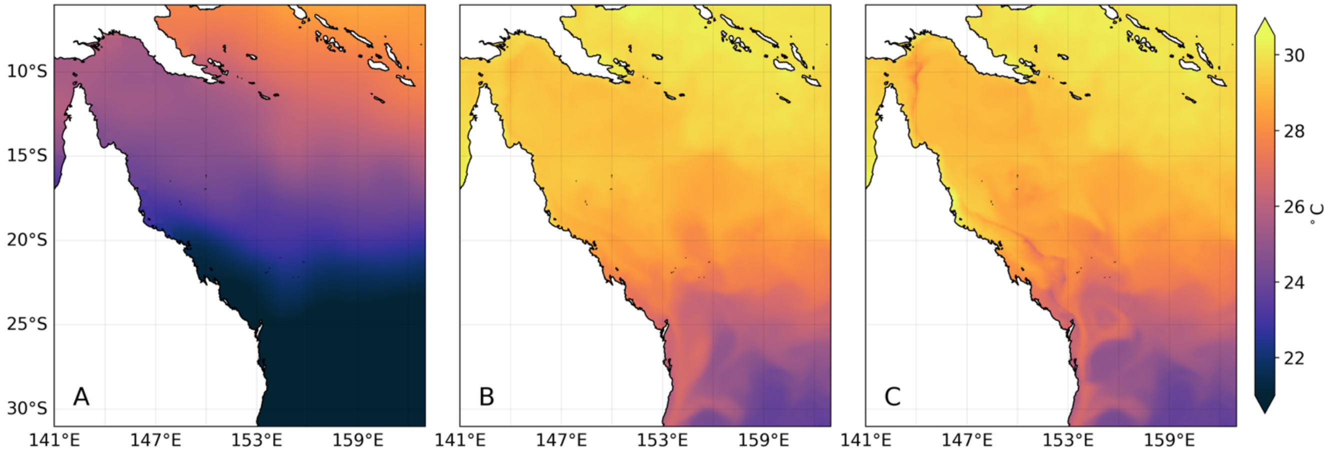

Figure 2. Sea surface temperature used to force the atmospheric NE AUS domain for February 2022 (time average) from the (A) HadISST monthly mean climatology, (B) daily mean BRAN2020 reanalysis used in ACCESS-GBR (atmosphere-only) and (C) the merged BRAN2020-GBR4 SST used in the coupled ACCESS-EMS-GBR configuration.

2.4.2 Coupled atmospheric fields

In the GBR4 model, atmospheric conditions are prescribed by outputs from the NE AUS domain at 0.04° horizontal grid-spacing. Hourly mean surface temperature, dew point, mean sea level pressure, horizontal winds, cloud fraction, total downwelling surface short-wave radiation (which is responsive to simulated aerosol and cloud) and hourly accumulated precipitation are provided as netcdf files and are interpolated onto the GBR4 grid by the SHOC code. To overcome problems arising in coastal grid boxes (e.g. where air temperature over a partial land cell can lead to overheating of coastal waters), all cells containing land are masked with the nearest ocean value. Using the NE AUS outputs provides several benefits, including representing the atmospheric state at a high spatial resolution, with good alignment between the atmospheric and

https://doi.org/10.5194/egusphere-2026-2761
Preprint. Discussion started: 16 July 2026

ocean model grids (~4 km grid-spacing), and the ability to customize atmospheric forcings depending on simulation requirements (e.g. to include aerosol deposition to the surface ocean).

3 Model evaluation

3.1 Simulations and evaluation metrics

The performance of the ACCESS-EMS-GBR model in simulating observed aerosol and seawater fields is assessed using measurements from in-situ monitoring networks and two recent field campaigns undertaken by RRAP-CS in February 2022 and March 2023. To coincide with the field campaigns, the model was run for 1-28 February 2022 and 1-31 March 2023. Validation of the simulated meteorology during these campaigns is provided in Appendix B.

The observational frequency varied between the campaigns and measurements. To best align the time-series of modelled and measured values and avoid instances where corresponding measurements were not available on the instantaneous time-step, the observations were averaged into an hourly time-series for comparison with the model. The hourly mean model outputs were extracted for the coordinates of each hourly mean in-situ observation, using linear interpolation for the regular atmospheric model grid and the nearest grid cell for the curvilinear ocean model.

Agreement between the modelled and measured variables is quantified using a range of metrics. The normalized mean bias factor (NMBF, Yu et al., 2006) provides a symmetric indication of bias, where a value of +0.5 and -0.5 indicates a respective over and under-estimate of a measured value by a factor of 1.5, and a value of 0 indicates perfect agreement. The mean absolute bias is provided to give further context to the magnitude of model biases, and Spearman's ranked correlation is used to assess coherence between the modelled and observed temporal trends. A summary of the in-situ datasets used for this analysis is provided in Table 2.

Table 2. Summary of in-situ datasets used to evaluate the ACCESS-EMS-GBR model

Dataset	Location	Measured variables*
RRAP-CS February 2022	Central GBR, between Townsville and Davies Reef (18.50 – 19.25°, 146.83 – 147.77°E)	N10 and CCN
RRAP-CS March 2023	Heron Island (23.44°S, 151.91°E)	N10, CCN, aerosol size distribution, aerosol composition (SO_4, BC, Organics)
AERONET	Lucinda (18.52°S, 146.39°E)	AOD
EcoRRAP Oceanographic loggers	Davies Reef: • Lagoon flat (18.833°S, 147.634°E)	Seawater temperature (0.5 m)

https://doi.org/10.5194/egusphere-2026-2761
Preprint. Discussion started: 16 July 2026

• Front shallow (18.819°S, 147.664°E)	Seawater temperature (3.8 m)
• Front deep (18.820°S, 147.664°E)	Seawater temperature and PAR (13 m)
Heron Island:	
• Lagoon shallow (23.454°S, 151.968°E)	Seawater temperature (5 m)
• Front shallow (23.470°S, 151.951°E)	Seawater temperature (5 m)
• Front deep (23.471°S, 151.951°E)	Seawater temperature and PAR (14.5 m)

*N10 = number concentration of aerosol with a dry diameter > 10 nm. CCN = number concentration of cloud condensation nuclei (assuming 0.2% supersaturation). AOD = aerosol optical depth. SO_4, BC, Organics = aerosol sulphate, black carbon and organic masses. PAR = photosynthetically active radiation.

3.2 Observations

3.2.1 RRAP-CS February 2022 field campaign

In February 2022, the RV *Guardian* and RV *Magnetic* travelled between Townsville and the central GBR near Davies Reef (18.83°S, 147.63°E) and Big Broadhurst Reef (18.91°S, 147.74°E). Testing of the seawater atomisation systems for MCB was occurring during this campaign on board the RV *Guardian*, while background atmospheric and sea spray plume-influenced measurements were made on board the RV *Magnetic*. Additional background aerosol measurements were made on board the RV *Guardian*, using equipment placed upwind of the sprayers. The modelled aerosol fields were interpolated to a height of 10 m, to match the height of the sampling inlets.

The number concentration of aerosol with dry diameter between 10 nm and 2.5 µm (N10, cm^{-3}) was measured at approximately 1 second intervals using a butanol Condensation Particle Counter (bCPC, AIRMODUS A20) on board the RV *Guardian* until 13 February. Additional measurements were made using a mixing Condensation Particle Counter (mCPC, Brechtel, upper detection limit of 2 µm) on board the RV *Magnetic* throughout the campaign. To exclude any potential ship exhaust artifacts, the aerosol dataset was filtered to include data only when wind direction was within a 180º frontal arc (270º to 90º) of the ship's heading, when wind speed relative to the ship speed was greater than 2 m s^{-1} and when particle counts were less than 10,000 cm^{-3}. The same filtering was applied to the modelled N10. Measurements were also excluded when sea spray emission activities were occurring on board the RV *Guardian* (for testing of the seawater atomisation systems for fogging and MCB).

The number concentration of cloud condensation nuclei (CCN, cm^{-3}) at 0.1%, 0.2%, 0.3%, 0.5% and 0.7% supersaturation (SS) was measured using a CCN counter (CCNc, CCN-100, Droplet Measurement Technologies) on board the RV *Magnetic* at 10-minute intervals for each SS. During a subsequent campaign in March 2023, measured CCN was dominated by accumulation mode aerosol, with only a small fraction of the Aitken mode activating (see Horchler et al., 2025 for a detailed analysis of the size distribution data, which are not included in this study). The near-surface level (10 m) modelled CCN number concentration was calculated for each measured supersaturation, assuming an activation dry diameter of ~32.1 nm at 0.7% SS to ~117.2 nm at 0.1% SS, representing a range of theoretical updraught conditions. While the model agreement across the range of measured SS conditions is assessed, biases in the time-series of modelled CCN are calculated at 0.1% SS, chosen to reflect the observed critical diameter of approximately 100 nm in both marine and continental air masses in March 2022 (Horchler et al., 2025). The aerosol measurements were made and processed by E. J. Horchler, J. Alroe, L. Cravigan, L. Harrison, Z. Ristovski and D. Harrison. Further details of the measurement methods on board the RV *Magnetic* are provided in Horchler et al. (2025).

3.2.2 RRAP-CS March 2023 field campaign

In March 2023, measurements of aerosol number concentration, size distribution and composition were made at the Heron Island Research Station (23.44°S, 151.91°E), approximately 5 m above sea level. N10 was measured using a Condensation Particle Counter (CPC 3782, TSI Inc., upper detection limit of 3 µm), while CCN was measured using a CCNc (CCN-100, Droplet Measurement Technologies).

As for 2022, the modelled CCN was calculated at 0.1%, 0.2%, 0.3%, 0.5% and 0.7% SS, with biases calculated for the modelled CCN at 0.1% supersaturation (see section 3.2.1). The aerosol size distribution was derived from measurements of total particle concentration and diameter (5-2000 nm), using measurements from a Scanning Electrical Mobility Spectrometer (SEMS, Brechtel Manufacturing Inc.) and Aerodynamic Particle Sizer (APS 3321, TSI Inc.).

The aerosol sulphate (SO_4) and total organic masses were measured with an Aerosol Mass Spectrometer (c-ToF-AMS, Aerodyne Research Inc.), and the BC concentration with an Aethalometer (AE33-7, Magee Scientific). Measurements of the aerosol sea salt mass were not available. Measurements were made and processed by E. J. Horchler.

The model output at 5 m above sea level was compared with the observations. The modelled organic carbon (OC) mass was converted to organic matter (OM) using the assumed ratio of OM:OC of 1.4. Similarly, the model outputs aerosol sulphate mass as sulfuric acid, which was converted to SO_4 by multiplying by the ratio of the molar masses for SO_4 and sulfuric acid (~0.974, as per Talvinen et al., 2025).

The AMS is most efficient at measuring the composition of particles in the 40 – 2000 nm diameter range, but detection beyond this range is possible. To best compare the observed and modelled aerosol masses (including beyond the most efficient detection size range), the modelled SO_4, organic and BC masses were summed over all aerosol modes, potentially spanning ~1.5 to > 5000 nm (Table 1) but with an upper limit of approximately 1100 nm during the March 2023 campaign (see Results).

https://doi.org/10.5194/egusphere-2026-2761
Preprint. Discussion started: 16 July 2026

3.2.3 AERONET

Radiometer measurements of aerosol optical depth (AOD) are available from the AERONET Lucinda site (18.52°S, 146.39°E) at approximately 10-minute intervals. Measured AOD for February 2022 and March 2023 were processed into an hourly mean time-series for comparison with the modelled AOD (550 nm). The measured AOD were obtained for the closest available wavelength (551 nm in February 2022, 532 nm for March 2023) to the modelled AOD, which was interpolated to a height of 8 m to align with the measurement elevation. The AERONET Level 2.0 data have undergone quality assurance with pre- and post-field calibration and are available from https://aeronet.gsfc.nasa.gov, along with details of the measurement equipment and processing algorithms.

3.2.4 EcoRRAP Oceanographic Logger data

In-situ measurements of physical seawater variables are available from a network of oceanographic loggers deployed as part of EcoRRAP, an RRAP sub-program that has involved the establishment of long-term monitoring sites throughout the GBR. At Davies Reef and Heron Island, seawater temperature loggers (RBRSolo3) are deployed at various reef zones and depths, with additional photosynthetically active radiation (PAR) sensors (Licor-192) and conductivity, temperature and depth (CTD) loggers deployed at the deeper reef front sites. Here, we compare the model outputs with measurements of seawater temperature (°C) at the 'shallow lagoon', 'shallow reef front' and 'deep reef front' monitoring sites (Table 2) at Davies Reef and Heron Island to assess the model skill in capturing local variability in temperature across reef zones, as well as PAR (mol m^{-2} s^{-1}) at the 'deep reef front' sites. The data are available from the AIMS Data Repository (https://apps.aims.gov.au/). Modelled seawater fields were interpolated to the respective depth of each monitoring site (Table 2).

4 Results

4.1 Aerosol number concentration

The measured N10 was characterised by terrestrially influenced air masses during the first week of the February 2022 campaign, when number concentration was often more than double the apparent marine background concentration observed from 15 February onwards (Fig. 3A). A similar trend was observed at Heron Island in March 2023, where the measured N10 periodically increased above the background around 4, 13 and 19 March (Fig. 3B). The high N10 events around 4 and 13 March 2023 were dominated by particles in the nucleation and Aitken mode, while the event around 19 March was dominated by larger particles.

https://doi.org/10.5194/egusphere-2026-2761
Preprint. Discussion started: 16 July 2026

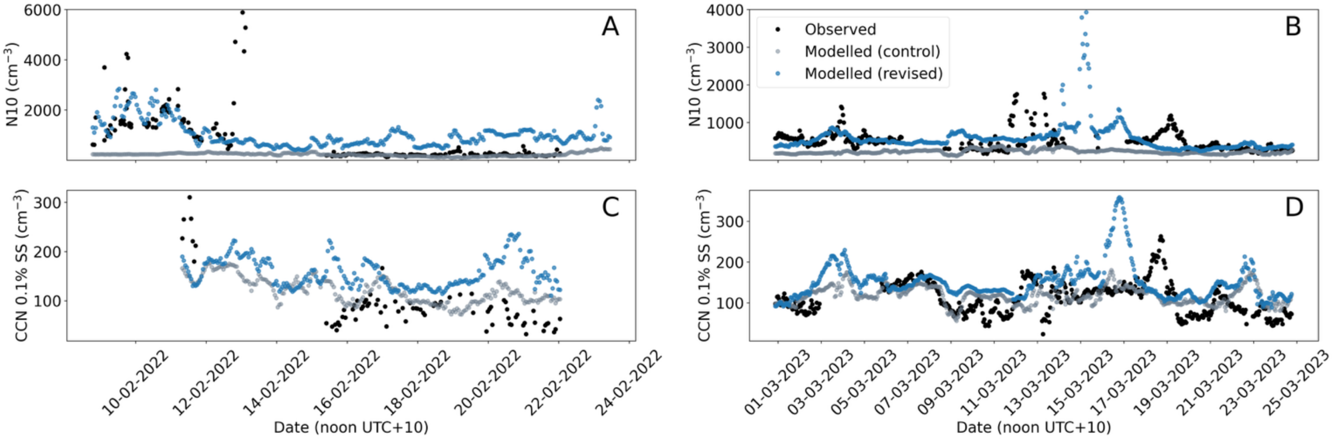

Figure 3. Measured and modelled hourly mean (top) N10 and (bottom) CCN, along the (left) RV *Guardian* and RV *Magnetic* ship tracks in February 2022 and (right) at the Heron Island Research Station in March 2023. Modelled values are shown for both the control and revised aerosol setup described in Sect. 2.1.2.

For the initial control ACCESS-EMS-GBR simulations, the model captured the background N10 relatively well however, strongly underestimated events where N10 became elevated above the background during both February 2022 (NMBF = -2.61, mean bias = -534.1 cm^{-3}, Fig. 3A) and March 2023 (NMBF = -1.24, mean bias = -275.3 cm^{-3}, Fig. 3B). Conversely, the model represented the measured CCN (0.1% SS) relatively well in February 2022 (NMBF = 0.25, mean bias = 22.6 cm^{-3}, Fig. 3C) and March 2023 (NMBF = 0.05, mean bias = 5.0 cm^{-3}, Fig. 3D), indicating that the model was initially missing sources of Aitken mode aerosol. A bimodal mean size distribution was observed at Heron Island in March 2023 (Fig. 4). The initial underestimate in simulated number concentration was particularly evident in the size distribution data, where the Aitken mode was largely missing from the model.

https://doi.org/10.5194/egusphere-2026-2761
Preprint. Discussion started: 16 July 2026

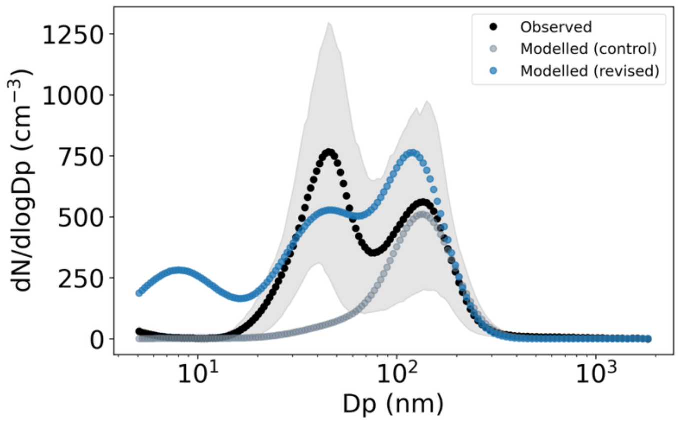

Figure 4. Measured and modelled aerosol size distribution at Heron Island as a time-average over the March 2023 campaign. The modelled size distribution is shown for both the control and revised aerosol setup described in Sect. 2.1.2. The shaded region indicates the 10th to 90th percentile range of the observed size distribution

After revising the aerosol emission sources and assumptions, and enabling BLN (see Sect. 2.1.2), the bias in N10 substantially improved (Fig. 3A-B). The changes contributed to a better representation of both the range and variability in observed N10 in February 2022 (NMBF = 0.36, mean bias = 269.5 cm^{-3}) and March 2023 (NMBF = -6.5x10^{-3}, mean bias = -3.2 cm^{-3}), including the periodic increases in number concentration from 8-14 February 2022 and around 4 and 13 March 2023. However, the low number concentration observed in late February 2022 was now overestimated, and the timing of the peak concentration around 19 March 2023 was missed by the model, indicating that further refinement of the emission sources and assumptions is needed to better capture short-term variability in aerosol over the GBR.

While the revised aerosol setup improved agreement between the modelled and observed N10, the revisions increased the model CCN (0.1% SS) bias in both February 2022 (NMBF = 0.74, mean bias = 67.3 cm^{-3}, Fig. 3C) and March 2023 (NMBF = 0.32, mean bias = 35.2 cm^{-3}, Fig. 3D). The revised mean aerosol size distribution shows improved agreement with observations (Fig. 4) however, the Aitken mode underestimate persists and the accumulation mode bias increased. While the Aitken and accumulation mode number concentrations increased, the modal mean diameters remained unchanged, suggesting that the changes predominately contributed to new particle formation and subsequent growth to the Aitken and accumulation modes, rather than condensational growth of pre-existing particles, in which a shift in the modal diameters would have also been expected.

Given that the shape and median diameter of the Aitken and accumulation modes are reasonably consistent between the observed and modelled size distributions (Fig. 4), it is plausible that new particle formation is correctly increasing the number of aerosol however, growth processes are causing too many particles to contribute to the accumulation mode, when a portion should instead remain in the Aitken mode.

https://doi.org/10.5194/egusphere-2026-2761
Preprint. Discussion started: 16 July 2026

Nonetheless, the model captures the measured CCN across the measured SS (representing a range of possible updraught conditions) reasonably well, particularly in March 2023 (Fig. 5). While the emission size assumptions and possibly the mode-merging processes in the aerosol scheme require further adjustment for the GBR region, the revised aerosol setup has substantially improved the model representation of total aerosol number concentration while adequately capturing CCN during the two field campaigns (Table 3).

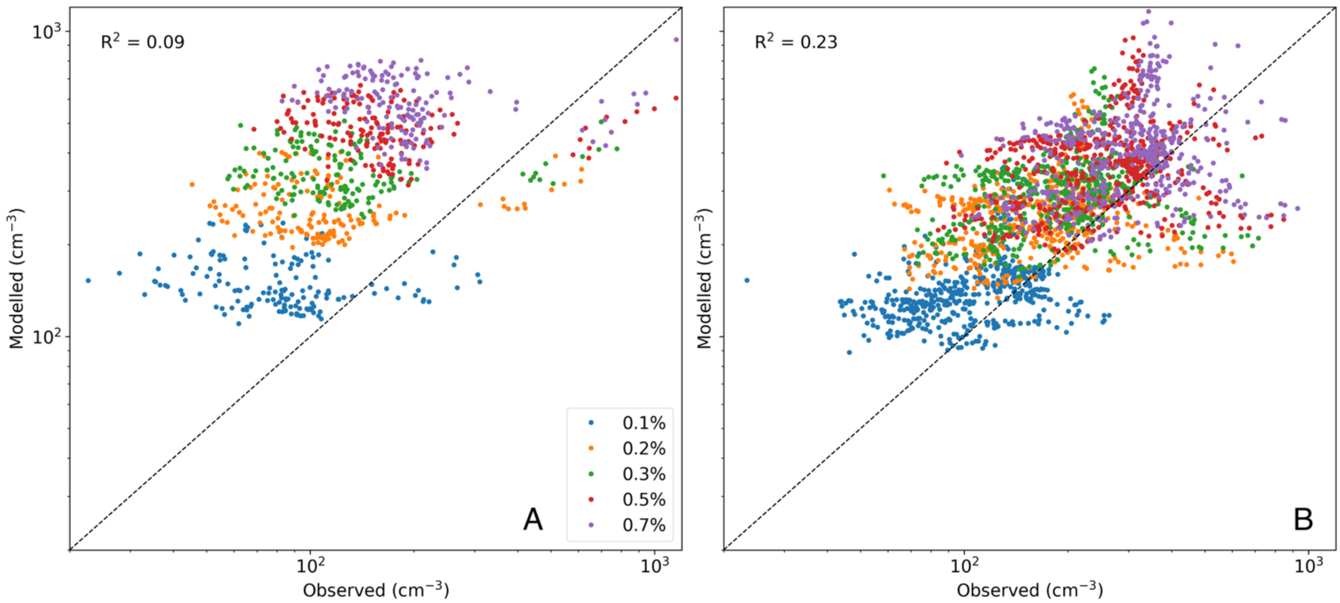

Figure 5. Observed versus modelled CCN at 0.1%, 0.2%, 0.3%, 0.5% and 0.7% supersaturation during the (A) February 2022 campaign in the central GBR and (B) March 2023 campaign at the Heron Island Research Station.

Table 3. Observed and modelled (control and revised) mean and model bias metrics for aerosol variables measured aboard the RV *Guardian* and RV *Magnetic* in February 2022 and at the Heron Island Research Station in March 2023.

Variable		February 2022 (RV *Guardian* and RV *Magnetic*)			March 2023 (Heron Island Research Station)		
		Mean (and model bias)	NMBF	Correlation	Mean (and model bias)	NMBF	Correlation
N10 (cm^{-3})	Observed	739.1 (n=176)	–	–	498.1 (n=436)	–	–
	Control	205.0 (-534.1)	-2.61	0.61 (p<0.001)	222.8 (-275.3)	-1.24	-0.08 (p=0.10)
	Revised	1008.6 (269.5)	0.36	0.37 (p<0.001)	494.9 (-3.2)	-6.5×10^{-3}	0.17 (p<0.001)
CCN	Observed	90.73 (n=78)	–	–	110.81 (n=500)	–	–

https://doi.org/10.5194/egusphere-2026-2761
Preprint. Discussion started: 16 July 2026

(cm^{-3})	Control	113.3 (22.57)	0.25	0.19 (p=0.09)	115.9 (5.0)	0.05	0.34 (p<0.001)
	Revised	158.0 (67.28)	0.74	-0.24 (p=0.03)	146.0 (35.2)	0.32	0.39 (p<0.001)
SO_4 ($\mu g\ m^{-3}$)	Observed	–	–	–	0.47 (n=572)	–	–
	Control	–	–	–	0.46 (0.004)	-8.9x10^{-3}	0.03 (p=0.47)
	Revised	–	–	–	0.56 (0.09)	0.19	0.21 (p<0.001)
Organics ($\mu g\ m^{-3}$)	Observed	–	–	–	0.29 (n=571)	–	–
	Control	–	–	–	0.28 (-0.018)	-0.07	0.34 (p<0.001)
	Revised	–	–	–	0.24 (-0.051)	-0.21	0.34 (p<0.001)
BC ($\mu g\ m^{-3}$)	Observed	–	–	–	0.019 (n=522)	–	–
	Control	–	–	–	0.012 (-0.007)	-0.55	-0.05 (p=0.23)
	Revised	–	–	–	0.016 (-0.003)	-0.19	-0.01 (p=0.75)
AOD	Observed	0.136 (n=179)	–	–	0.070 (n=121)	–	–
	Control	0.126 (-0.01)	-0.08	0.27 (p<0.001)	0.098 (0.029)	0.41	0.14 (p=0.13)
	Revised	0.132 (-4.5x10^{-3})	-0.03	0.35 (p<0.001)	0.087 (0.017)	0.25	0.18 (p=0.045)

4.1.1 Aerosol composition

Aerosol composition was also measured at Heron Island during the March 2023 campaign. For the initial control simulations, the model represented observed aerosol SO_4 (NMBF = -8.9x10^{-3}, mean bias= 0.004 μm^{-3}, Fig. 6A), organic (NMBF = -0.07, mean bias = -0.018 μm^{-3}, Fig. 6B) and BC (NMBF = -0.55, mean bias = -0.007 μm^{-3}, Fig. 6C) masses well. Revising the aerosol setup (see Sect. 2.1.2) did not improve biases in the modelled aerosol sulphate and organic masses however, the magnitude of biases remained small (absolute NMBF $\leq$ 0.22, absolute mean bias $\leq$ 0.10 μm^{-3}, Table 3).

https://doi.org/10.5194/egusphere-2026-2761
Preprint. Discussion started: 16 July 2026

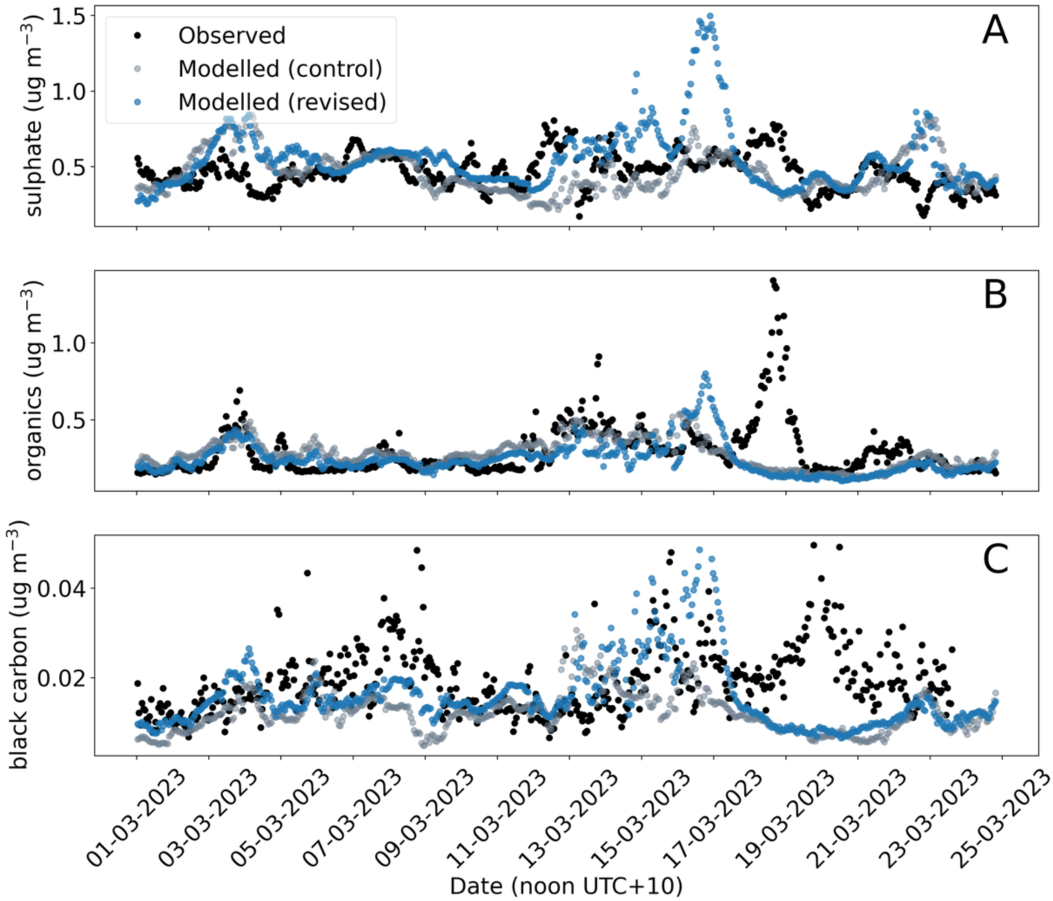

505

Figure 6. Measured and modelled aerosol (A) sulphate, (B) organic and (C) black carbon mass at the Heron Island Research Station in March 2023. The modelled concentrations are shown for both the control and revised aerosol setup described in Sect. 2.1.2.

The observed sulphate and organic masses closely aligned with the CCN time-series (Fig. 3D), indicating a strong influence of organics (as secondary organic aerosol, primary marine organics and/or other terrestrial sources) and sulphate (as non-sea salt sulphate from the oxidation of DMS and/or anthropogenic sources) on CCN composition over the GBR. The peak in observed N10 on 19 March 2023 was also evident in the SO_4, organic and BC aerosol masses, and in the model, although occurred approximately 48 hours earlier in the model. The magnitude of the peak in SO_4 aerosol mass was overestimated, leading to an overall positive model bias (Table 3).

The offset in the timing and magnitude of sporadic emission events (such as the observed peak in aerosol number concentration and masses on 19 March 2023) may be due to a number of factors, including the overestimate of wind speed in the model at the sheltered Heron Island Research Station (particularly from 17 March 2023, see Appendix B) or point source

https://doi.org/10.5194/egusphere-2026-2761
Preprint. Discussion started: 16 July 2026

emissions that may not be fully captured at the spatial and temporal resolution of the atmospheric model. While there is room for improvement, the model captured the observed variability in aerosol composition well (Table 3), including at the diurnal scale, which can be difficult to model from monthly mean emission fields. Although, the model accounts for some diurnal variability by scaling the offline oxidant monthly mean fields to 'mimic' the diurnal cycle.

4.1.2 Aerosol optical depth

Measured AOD at the AERONET Lucinda site was highly variable, ranging from 0.07 – 0.29 (mean 0.14) in February 2022 and 0.04 – 0.11 (mean 0.07) in March 2023 (Fig. 7). The control simulation captured this variability well during both campaigns (Fig. 7), with occasional biases in the hourly datasets leading to respective NMBF values of -0.08 and 0.41. The revised aerosol setup improved agreement with observed AOD (mean bias <0.02, Table 3), with the NMBF reducing to -0.03 in February 2022 and 0.25 in March 2023, indicating reasonable agreement with the observations.

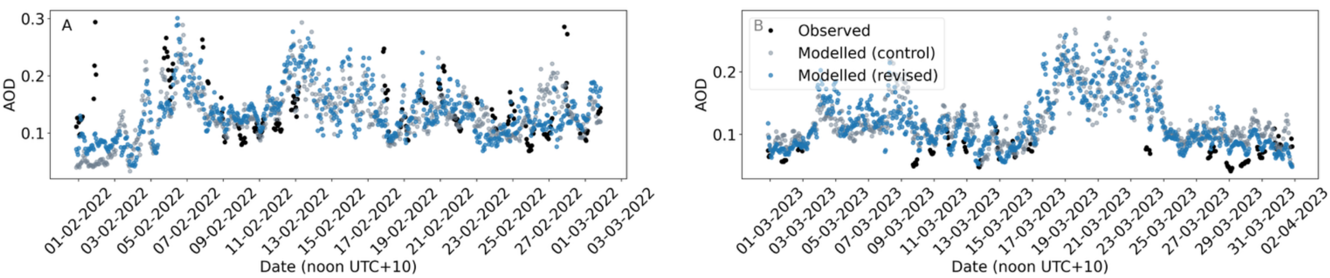

Figure 7. Measured and modelled aerosol optical depth (AOD) at the AERONET Lucinda site in (A) February 2022 and (B) March 2023.

4.2 Seawater temperature and PAR

The modelled seawater temperature across the shallow lagoon, reef slope and deep sites were broadly consistent with observations from the EcoRRAP monitoring sites at Davies Reef and Heron Island (Fig. 8). The mean and overall trends in SST were captured by the model in 2022 and at Heron Island in 2023, although diurnal variability in observed temperature was more variable. Bathymetry and hydrodynamic processes (such as heating of shallow lagoon waters and upwelling along the reef slope) influence seawater temperature across the reef zones at sub-kilometre scales, which are not expected to be fully-resolved by the GBR4 model (~4 km horizontal grid spacing).

https://doi.org/10.5194/egusphere-2026-2761
Preprint. Discussion started: 16 July 2026

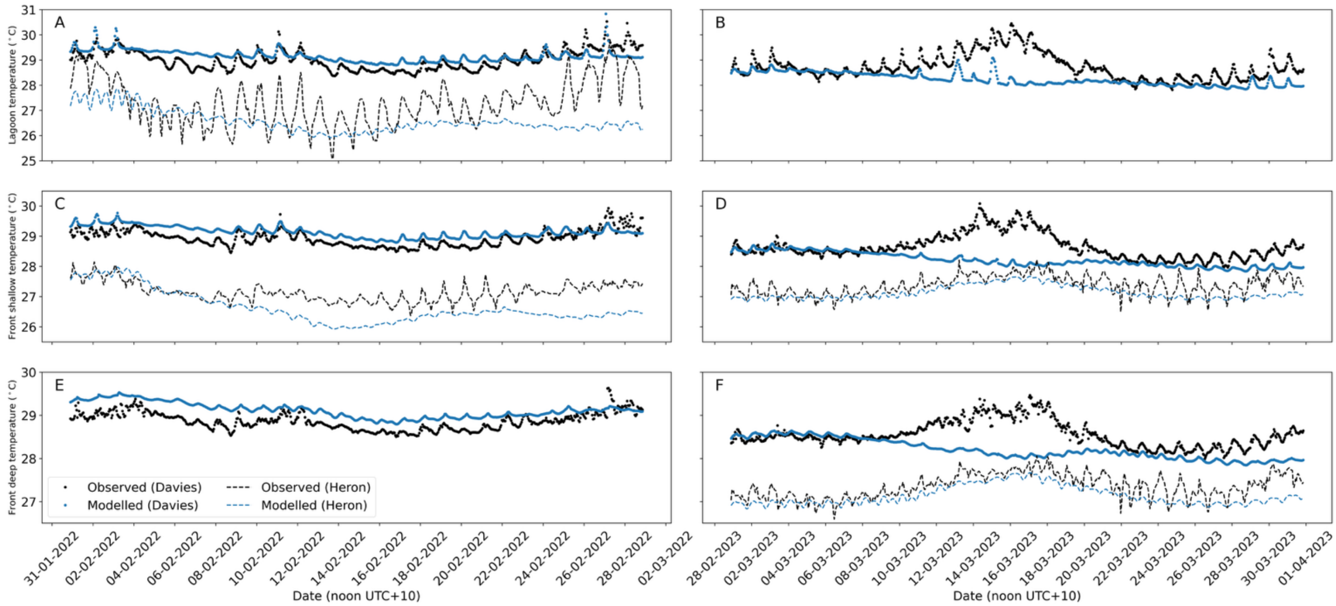

Figure 8. Measured and modelled hourly mean seawater temperature at the Davies Reef (solid) and Heron Island (dashed) EcoRRAP monitoring sites situated in the (top) shallow lagoon, (middle) shallow reef front and (bottom) deep reef front zones. No temperature data was available from the Heron Island deep reef front site in February 2022 or lagoon site in March 2023.

Temperature was highly variable at the Heron Island lagoon site in February 2022, with a diurnal range of > 2°C on most days in the lead up to the 2022 mass coral bleaching event (Fig. 10A). While the model underestimated the full diurnal range at this site, the means were generally consistent until late February 2022, after which doldrum conditions (increased air temperature and low winds; Fig. B1) contributed to warming of the shallow reef waters, particularly in the lagoon (Fig. 10A). Similarly, a warming event was observed in mid-March across all reef zones at both locations (Fig. 8B, D, F). The increase in temperature was captured by the model at Heron Island but underestimated at Davies Reef. Despite the local variability across reef zones not being fully captured by the GBR4 model, the bias metrics indicate good overall agreement between the measured and modelled seawater temperature with latitude and depth (absolute mean bias ≤ 0.72°C, absolute NMBF < 0.03 and statistically significant correlations at p<0.001, Table 4).

Table 4. Observed and modelled mean and model bias metrics for seawater temperature (°C) and PAR (mol m^{-2} hr^{-1}) at Heron Island and Davies Reef lagoon, shallow reef front and deep reef front monitoring sites in February 2022 and March 2023.

		2022				2023			
Variable	Site^{+}	Observed	Modelled	NMBF	Correlation*	Observed	Modelled	NMBF	Correlation*
Temperature (°C)	Heron lagoon	27.29	26.57 (-0.72)	-0.027	0.35	–	–	–	–
	Heron shallow	27.14	26.64 (-0.51)	-0.019	0.56	27.38	27.14 (-0.24)	-0.009	0.78
	Heron deep	–	–	–	–	27.36	27.14 (-0.22)	-0.008	0.81
	Davies lagoon	29.01	29.17 (0.15)	5.3x10^{-3}	0.71	28.73	28.24 (-0.49)	-0.018	0.35
	Davies shallow	28.94	29.15 (0.21)	7.3x10^{-3}	0.77	28.64	28.22 (-0.42)	-0.015	0.27
	Davies deep	28.86	29.12 (0.25)	8.8x10^{-3}	0.78	28.55	28.21 (-0.35)	-0.012	0.23
PAR (mol m^{-2} hr^{-1})	Heron deep	0.30	0.32 (0.02)	0.054	0.91	0.32	0.26 (-0.06)	-0.25	0.87
	Davies deep	0.37	0.49 (0.12)	0.33	0.87	0.32	0.45 (0.13)	0.41	0.91

*All correlation coefficients are statistically significant at $p<0.001$. $^{+}$At Heron Island and Davies Reef, n=672 in 2022 and n=744 in 2023.

Simulated PAR at the EcoRRAP reef front sites was also consistent with observations for most of the 2022 and 2023 campaigns (Fig. 9), with an absolute NMBF $\leq$ 0.41 and Spearman's correlation coefficient $\geq$ 0.87 ($p<0.001$) indicating moderate agreement between the measured and modelled PAR (Table 4). At Davies Reef, the midday peaks in underwater PAR were often overestimated by the model, although the mean bias was low (< 0.13 mol m^{-2} hr^{-1}). Conversely, the midday peaks at Heron Island were occasionally underestimated, particularly during the warm period in mid-March 2023 (Fig. 9D). The PAR sensors are situated at a depth of approximately 13 m at Davies Reef and 14.5 m at Heron Island, representing light near corals. The PAR biases may be due to small-scale differences in sea surface albedo and water column composition along the reef slopes that are not fully represented in the GBR4 model. Even so, the overall mean and daily variability are captured, indicating that the model adequately represents irradiance, both at the surface and attenuated through the water column.

https://doi.org/10.5194/egusphere-2026-2761
Preprint. Discussion started: 16 July 2026

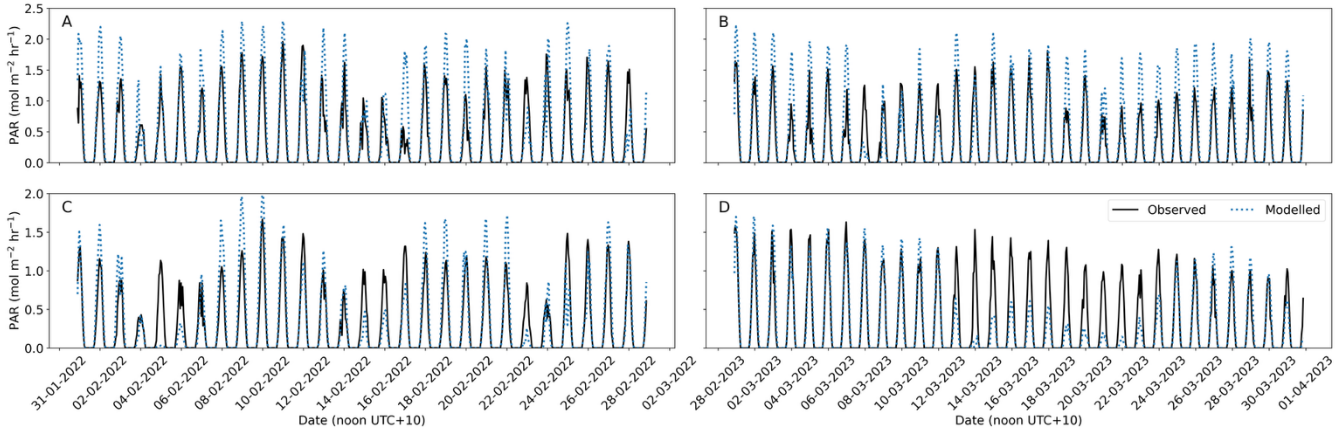

Figure 9. Measured and modelled hourly mean photosynthetically active radiation (PAR) at the EcoRRAP deep reef front monitoring sites at (top) Davies Reef and (bottom) Heron Island in (left) February 2022 and (right) March 2023.

5 Discussion

The ACCESS-EMS-GBR model described here was designed to assess the feasibility and impacts of MCB in the GBR, which has been suggested as a way mitigate the severity of coral bleaching. Several atmospheric models are needed to assess the efficacy and impacts of MCB, covering spatial scales ranging from cloud parcel models to assess impacts at the cloud microphysical scale, to global models to assess the large-scale impacts. The ACCESS-EMS-GBR model can assess impacts at global to regional (~4 km horizontal resolution) scales, with the added capability of simulating impacts in the underlying coral reef and capturing feedbacks due to changes in heat fluxes at the sea surface.

The model is unique in that it is the first regional model to represent detailed aerosol, cloud microphysics and radiative processes in the atmosphere, as well as hydrodynamics, biogeochemical properties, ecology and coral reef processes in the marine environment. Fluxes of heat, moisture and radiation between the atmosphere and sea surface are captured, with subsequent effects on mixing and ecological processes in the ocean (e.g. through changes in temperature and light) also represented.

The model captures measured meteorology, aerosol and seawater temperature and PAR reasonably well in the GBR. The revised aerosol setup described in Sect. 2.1.2 substantially improved the initial bias in simulated aerosol number concentration. The improvement in N10 was largely due to the inclusion of organic-mediated BLN, forming new particles at a rate that is determined by the concentration of gas-phase sulfuric-acid and secondary organic species (Metzger et al., 2010), derived from the oxidation of monoterpenes. Revising the monoterpene emission source to represent emissions from terrestrial vegetation (which are an order of magnitude larger than anthropogenic emissions by mass over north-eastern

https://doi.org/10.5194/egusphere-2026-2761
Preprint. Discussion started: 16 July 2026

Australia) increased sources of secondary organics in the model, contributing to new particle formation and subsequent growth to the Aitken and accumulation modes.

The strong influence of terrestrial secondary organics on particle number concentration is surprising over the GBR, given the dominance of south-easterly trade winds during both campaigns (see Appendix B). It is possible that interpolation of the coarse resolution (N216) global monoterpene emissions onto the regional NE AUS grid led to some overlap at the land-sea boundary, close to Heron Island and Davies Reef. While BLN correctly increased simulated N10, the BLN rate should perhaps be influenced by both marine and terrestrial organic sources and could improve the model agreement with sporadic emission events observed during both campaigns. Nonetheless, the results support previous findings that aerosol over the GBR is influenced by organic emissions transported from Queensland in both marine and continental influenced air masses (Horchler et al., 2025; Mallet et al., 2016).

While enabling BLN with the revised aerosol emissions and assumptions improved the model agreement with observed N10, biases in the Aitken and accumulation mode number concentrations persist, leading to an overestimate of CCN. The changes led to an increase in the Aitken and accumulation mode particle number concentrations but not the modal mean diameters, suggesting that new particle formation and growth dominated over the condensational sink, in which a shift in the modal diameters would have also been expected.

Similarly, Duncan et al. (2026) found that the modelled aerosol size distribution in the UK Earth System Model (UKESM) v1.0 (UKESM1.0, which uses the same aerosol scheme in a global configuration) responded to a volcanic emission event (producing high concentrations of Aitken mode aerosol) by increasing the Aitken and accumulation mode particle number concentration without significant growth of the mean diameter of either mode. When organic mediated BLN was enabled in UKESM1.0, the volcanic emission event increased both the accumulation mode mean diameter and particle number concentration, indicating that BLN contributed to both the mass of pre-existing aerosol and the number of aerosol particles. Our results align closely with the UKESM1.0 case study without BLN, possibly reflecting the reduced SOA yield and thus, BLN rate in the GBR simulations, leading to an overall increase in particle concentration rather than mass of pre-existing aerosol.

He et al. (2026) demonstrate that UKESM1.1 underestimates the Aitken mode (as was observed over the GBR), despite overestimating concentrations of aerosol precursors, and suggest that the Aitken mode bias is due to missing new particle formation pathways (such as marine boundary layer nucleation), involving species such as marine organic vapours. As discussed above, the organic concentrations that drive the organic-mediated BLN rate in GLOMAP-mode are entirely derived from terrestrial monoterpenes. However, the coral reef is also a source of organic vapours (Deschaseaux et al., 2025) that are not currently represented in the model.

Another possible source of bias in the Aitken and accumulation mode number concentrations is the terrestrial emission size assumptions. Currently, organic and black carbon emissions from biofuel and biomass burning are assumed to have a mean

https://doi.org/10.5194/egusphere-2026-2761
Preprint. Discussion started: 16 July 2026

dry diameter of 150 nm (Stier et al., 2005) and thus contribute primarily to the accumulation mode. Several studies report biomass burning emissions with geometric mean diameters ranging from approximately 30-160 nm (L. Chen et al., 2019; Pokhrel et al., 2021; Reid et al., 2005), with size depending on measurements of fresh or aged smoke, flaming or smouldering combustion and vegetation type, with one study reporting eucalypt burning emissions in the ~30-50 nm size range (Pokhrel et al., 2021). Similarly, several studies report biofuel emission size distributions with median dry diameters ranging from approximately 50-150 nm, depending on biofuel type (Di et al., 2010; Tiwari et al., 2014). The emission size assumptions in the model could reasonably be adjusted so that a larger portion contributes to the Aitken mode.

The effect of such model and aerosol emission adjustments on the simulated aerosol size distribution will be investigated as part of ongoing model sensitivity studies and developments. Future iterations of the model will also use a later version of the UM that includes updates to reflect recent science, including a bug fix for the calculation of hygroscopicity in the aerosol scheme (see UKCA Ticket #106).

Biases in the modelled accumulation mode and CCN number concentration can be improved however, the revised aerosol setup presented here is considered to be a good compromise for future MCB studies over the GBR. While CCN are the most relevant aerosol class for assessing impacts to cloud properties, the total aerosol load is also important in determining the rate of condensational growth and thus, the number of particles reaching the CCN activation size.

While no assessment of clouds is presented here, the reasonably good agreement of surface-level CCN at a range of supersaturations (representing a range of possible updraught conditions) suggests that the model can adequately capture cloud droplet number concentration, particularly with the revision of the Abdul-Razzak and Ghan (2000) activation scheme (Ghosh et al., 2025). The model also reproduced underwater PAR at a depth of approximately 15 m at Heron Island and Davies Reef reasonably well, suggesting that cloud cover and microphysical properties are adequately captured.

A detailed evaluation of cloud properties will be presented in future work alongside an assessment of the impacts of sea spray aerosol emissions for MCB on clouds, precipitation, radiation, temperature and ecological processes in the coral reef. The potential for MCB to mitigate coral bleaching will be assessed by quantifying changes in physical metrics such as Degree Heating Weeks (Liu et al., 2006) and simulated variables such as the concentration of reactive oxygen species in corals (Ellis et al., 2025) which can contribute to oxidative damage and bleaching (Lesser, 2011).

The capabilities of ACCESS-EMS-GBR make it well suited for studying various other ocean-atmosphere processes in the GBR, such as the impact of changes in temperature on precipitation or tropical cyclone intensity over the coral reef and north-eastern Australia. The model also provides the foundation for development of a regional earth system model. A regional earth system model, with representation of atmospheric dynamics and composition, and physical and biological processes in the coral reef, would enable numerous detailed studies of the GBR region.

Further work is needed to expand the atmosphere and ocean coupling to include other fields, such as the deposition of dust and black carbon from the atmosphere, which can influence nutrient concentrations in the ocean. Emissions of marine

https://doi.org/10.5194/egusphere-2026-2761
Preprint. Discussion started: 16 July 2026

aerosol (e.g. primary marine organics) and precursors (e.g. DMS) can also be coupled by prescribing sea surface concentrations simulated by the GBR4 model. The more accurate the prescribed emission fields are, the better the model is able to simulate aerosol fields (and subsequent impacts on clouds and radiation), as is demonstrated in the Results. Emissions of aerosol and precursors are currently simulated using monthly mean fields in ACCESS-EMS-GBR. While the model adequately captures measured aerosol over the GBR, the model skill in capturing sporadic, short-term variations in aerosol fields (such as changes in non-sea salt sulphate aerosol due to DMS emissions from the coral reef; Swan et al., 2017) could be further improved by refining the emission sources.

Further work is also needed to reduce the time-lag between the atmosphere and ocean models in ACCESS-EMS-GBR. This could be achieved by increasing the coupling frequency (e.g. from daily to 12-hourly), with an added computational cost, or by extrapolating the coupled sea surface fields forward through time. Alternatively, a more sophisticated coupling approach could be implemented, using a dedicated coupling system such as the Ocean Atmosphere Sea Ice Soil Model Coupling Toolkit (OASIS3-MCT), used to couple the global ocean and sea ice models in the ACCESS Ocean Model (ACCESS-OM2, Kiss et al., 2020), or its successors.

A dynamic catchment model could also be incorporated into the GBR4 model. Currently, freshwater inputs into the GBR are prescribed by outputs from the Dynamic SedNet catchment model (Ellis, 2018; McCloskey et al., 2021). Coupling the catchment model would allow freshwater flows to respond to any possible changes in precipitation simulated by the atmospheric model, as can occur with changes in aerosol emissions or convective processes.

There is also potential to include higher-resolution nested domains in both the atmosphere and ocean models. The RNS allows for one-way nesting of multiple limited area domains, with progressively smaller grid-box spacing (down to ~100 m). Additional regional domains could be nested within NE AUS, with kilometre-scale grid-spacing over small regions of the GBR. The eReefs modelling system also includes a higher-resolution GBR1 configuration (~1 km grid-spacing) that may be nested within GBR4. The higher-resolution atmospheric and ocean models are computationally expensive to run but can provide detailed information on local-scale processes over the coral reef, such as variability in light, temperature and coral bleaching.

While development of a regional earth system model is an aim for future work, the simple and flexible coupling approach currently used in ACCESS-EMS-GBR minimises developmental overhead and meets the requirements for simulating the MCB intervention. The model configuration described here will therefore be used for sensitivity studies, to identify the optimal sea spray aerosol emission scenario for achieving a surface cooling effect over the GBR, while minimising the magnitude of sea spray aerosol emissions and the potential for unintended consequences over north-eastern Australia.

https://doi.org/10.5194/egusphere-2026-2761
Preprint. Discussion started: 16 July 2026

6 Conclusions

The ACCESS-EMS-GBR coupled atmosphere-ocean model is a valuable tool for studying ocean and atmosphere processes in the GBR region. Distinctive features of the model are its detailed representation of the dynamics and composition of the atmosphere and the marine environment as well as ecological processes in the coral reef. In this paper, we have described the setup of the regional atmosphere and ocean models and the coupling framework, and evaluated the model skill in simulating measured atmospheric and seawater variables in the GBR. The model simulates measured meteorology, aerosol and seawater temperature and PAR reasonably well. Biases in simulated aerosol were improved by revising the emission sources and assumptions, and by enabling new particle formation via organic-mediated boundary layer nucleation, highlighting the importance of capturing regional emission sources and processes in high-resolution models. These model revisions enable the simulation of MCB over the GBR. Although, further work is needed to investigate the aerosol emission size assumptions in the model, with tuning likely needed to better represent the aerosol size distribution over the GBR region. The model provides the foundation for development of a regional earth system model, with pathways for future development provided in the Discussion. A regional model with coupled aerosol-cloud microphysics and representation of marine biogeochemistry and the coral reef ecosystem would be an innovative tool for atmosphere-ocean research.

Appendix A: Surface heat fluxes

An important consideration in coupling the atmospheric and ocean models is ensuring that heat fluxes are balanced. In the GBR4 hydrodynamic model, sensible and latent heat fluxes are parameterised and are proportional to the temperature gradient across the atmosphere and sea surface, which is influenced by near-surface winds, humidity, precipitation and solar radiation, all of which are prescribed by the atmospheric model.

In the atmospheric model, radiation is simulated by the SOCRATES scheme. Radiative transfer is represented in six short-wave bands and nine long-wave bands, which respond to concentrations of gas-phase species (such as greenhouse gases and water vapour), aerosol and clouds to simulate the total amount of SWR at the surface. Sensible and latent heat fluxes are derived in a similar manner to the hydrodynamic model, using the air-sea surface temperature gradient (derived from simulated air temperature and prescribed SST), wind stress and the gridbox mean surface transfer coefficients for heat and moisture for ocean grid boxes.

Heat fluxes are balanced as best as possible in the coupled model by exchanging atmospheric (radiation, cloud cover, winds, dew point, precipitation) and ocean fields (SST) that are used to derive heat fluxes between each model. In summer, a net loss of heat from the ocean to the atmosphere typically occurs over the shallow, warm waters of the GBR lagoon (Fig. A1), where evaporation can affect humidity and convective processes (McGowan et al., 2022). Conversely, a net positive heat flux can occur along the continental shelf in both the atmospheric and ocean models, largely driven by a smaller latent heat flux due to upwelling of cooler waters. The shift towards a net positive heat flux was particularly evident in late February

https://doi.org/10.5194/egusphere-2026-2761
Preprint. Discussion started: 16 July 2026

2022, when the magnitude of latent heat fluxes decreased, coinciding with the onset of doldrum conditions (characterised by low wind speeds, less latent heat flux and rapid warming of the reef) in the lead up to the 2022 mass coral bleaching event.

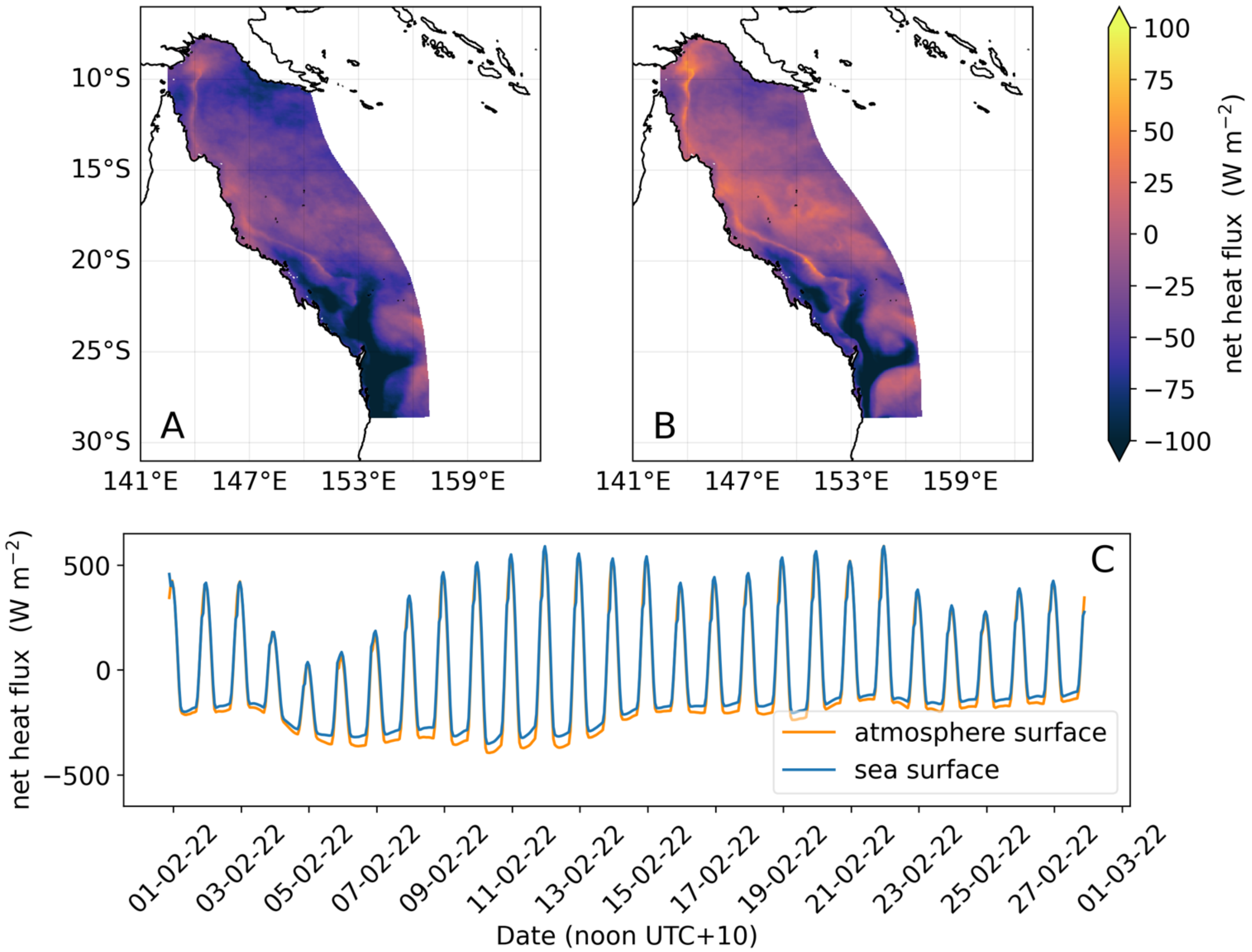

Figure A1. ACCESS-EMS-GBR simulated surface net heat flux in February 2022, simulated by the (A) atmospheric model and (B) the ocean model as a time-average and (C) as a time-series area-averaged over the GBR4 domain. Air to sea heat fluxes are positive, while losses of heat from the ocean to the atmosphere are negative.

The magnitude of net heat fluxes are approximately balanced in the atmospheric and ocean models, with both spatial and temporal variability aligning within the GBR4 domain (Fig. A1). Small differences in surface downwelling long-wave radiation, latent and sensible heat fluxes are present, in part due to small differences in the model grid box area between the atmosphere (regular grid) and ocean models (curvilinear grid). For example, 10 W m^{-2} of surface solar radiation at Heron Island (-23.44°S, 151.91°E) is equivalent to 181.35 mW when integrated over the closest atmospheric grid box (18.14 km^2) and 187.89 mW when integrated over the GBR4 grid box at the same location (18.79 km^2). Small differences in the net heat flux are also expected when using the lagged SST to force the atmospheric model (resulting in lagged effects of SST on sensible and latent heat fluxes in the atmosphere), and possibly due to differences in the parameterisations used to calculate surface heat budgets in the atmospheric and ocean models. Although, keeping the inputs to these parameterisations consistent where possible should minimise the impact of such limitations.

While this may be problematic for climate simulations (over years to decades), where small imbalances can propagate and induce artificial trends, the purpose of the regional domain is to provide information over short time-scales of days to months (e.g. to simulate a coral bleaching event). Further, heat fluxes are constrained in the models at the domain boundaries and during re-initialisation of the atmospheric model from the global nudged simulation, preventing imbalances from amplifying significantly through time.

Appendix B: Validation of simulated meteorology

The Australian Institute of Marine Science (AIMS) Northern Australia Automated Marine Weather and Oceanographic Stations provide measurements of air temperature (°C), pressure (hPa), wind speed (m s^{-1}) and wind direction (degrees). These data were obtained from an automated weather station (AWS) at Davies Reef (18.83°S, 147.63°E) and Heron Island (23.44°S, 151.91°E) for February 2022 and March 2023 (Australian Institute of Marine Science, 2020). Modelled meteorological fields were interpolated to a height of 10 m and 6 m above sea level for consistency with the observed meteorological data at Davies Reef and Heron Island, respectively. These data are available from the AIMS Data Repository (https://apps.aims.gov.au/). No meteorological data was available from the AIMS Heron Island weather station in March 2023. However, an automated weather station was operating on the Heron Island Research Station during the March 2023 field campaign. The meteorological measurements at the Heron Island Research Station are instead compared with the modelled meteorology in March 2023.

The model reproduced the observed meteorology well at both Heron Island and Davies Reef during the February 2022 and March 2023 campaigns (Fig. B1). At Heron Island in 2022, modelled air temperature (NMBF = -4.4×10^{-3}, mean bias = -0.12°C), air pressure (NMBF = -2.0×10^{-4}, mean bias = -0.19 hPa) and wind speed (NMBF = 0.01, mean bias = 0.1 m s^{-1}) were consistent with observations, with less than 1.2% difference between the modelled and observed means, and correlation coefficients that are statistically significant at $p<0.01$ (Table B1). Modelled wind direction was biased East during the first three days of February 2022, although was consistent with observations for the remainder of the campaign (mean bias = -15.62 degrees).

https://doi.org/10.5194/egusphere-2026-2761
Preprint. Discussion started: 16 July 2026

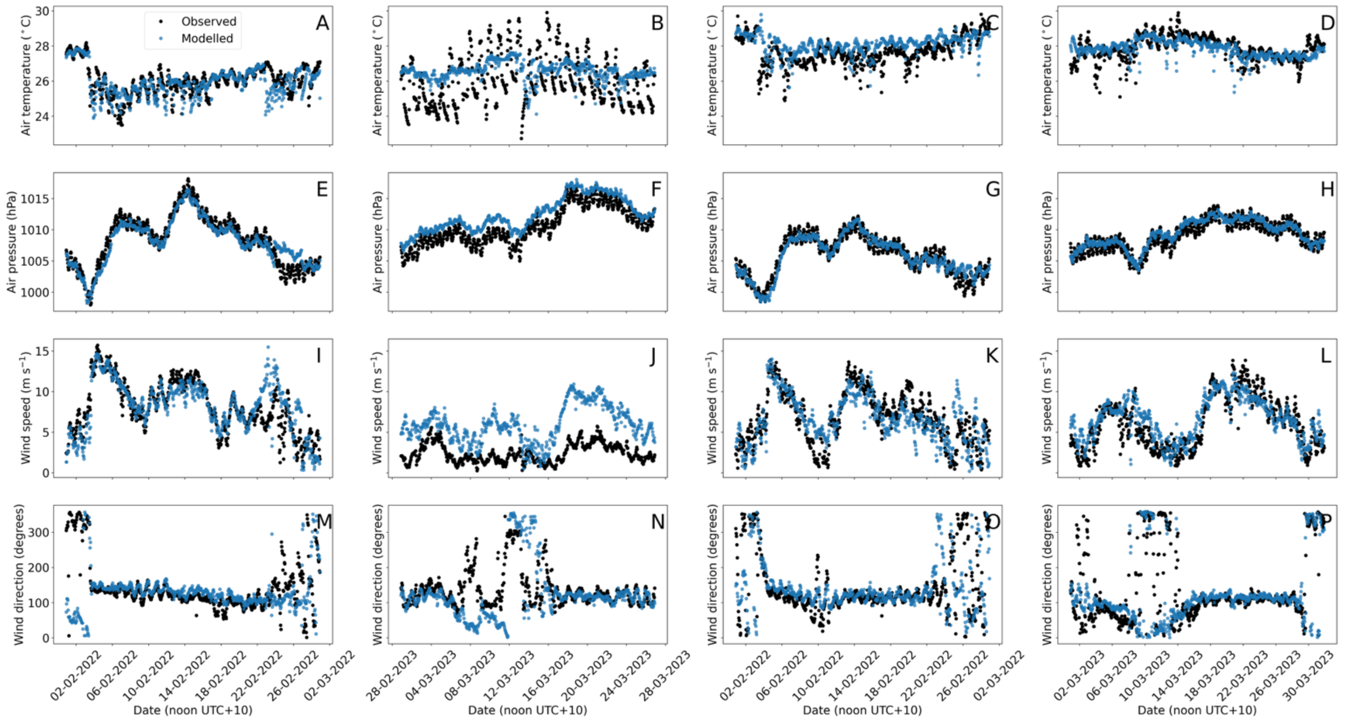

Figure B1. Measured (black) and modelled (blue) hourly mean air temperature, air pressure, wind speed and wind direction at (left) the AIMS Heron Island AWS in February 2022 and (left-centre) the Heron Island Research Station in March 2023, and at the AIMS Davies Reef AWS in (right-centre) February 2022 and (right) March 2023.

At the Heron Island Research Station in March 2023, the model reproduced air temperature (NMBF = 0.02, mean bias = 0.61°C), air pressure (NMBF = 1.8×10^{-3}, mean bias = 1.87 hPa) and wind direction (mean bias = -14.19 m s^{-1}) reasonably well, but overestimated wind speed (NMBF = 1.50, mean bias = 3.55 m s^{-1}). The Heron Island Research Station is more sheltered than the AIMS AWS, which is situated on the exposed eastern side of the reef. The horizontal grid spacing of the atmospheric model makes it best suited to capturing the more exposed conditions and may explain the poorer overall agreement between the measured and modelled meteorology at the Heron Island Research Station in March 2023.

At Davies Reef, modelled air temperature and air pressure had very good agreement with observations in February 2022 and March 2023 (NMBF < 0.02), again with less than 2% difference between the modelled and observed means and statistically significant correlation coefficients (Table B1). Modelled wind speed (NMBF < $\pm$0.09) and direction (mean bias < -20 degrees) were also well represented (Table B1). The diurnal range of air temperature and air pressure were not fully captured at Davies Reef, possibly reflecting small-scale convective processes that are not captured at the ~4 km horizontal grid spacing of the atmospheric model. However, the overall variability in simulated meteorology was consistent with observations (Table B1).

Table B1. Observed and modelled mean and model bias metrics for meteorological variables at Heron Island and Davies Reef in February 2022 and March 2023.

Variable	Metric	Heron Island 2022	Heron Island 2023	Davies Reef 2022	Davies Reef 2023
Air temperature	Observed mean (°C)	26.03 (n=672)	25.97 (n=620)	27.65 (n=669)	27.86 (n=726)
	Modelled mean (and bias, °C)	25.91 (-0.12)	26.58 (0.61)	28.10 (0.45)	27.82 (-0.04)
	NMBF	$-4.4x10^{-3}$	0.02	0.016	-0.002
	Correlation*	0.65	0.40	0.57	0.54
Air pressure	Observed mean (hPa)	1008.37 (n=667)	1010.55 (n=620)	1005.81 (n=666)	1009.06 (n=720)
	Modelled mean (and bias, hPa)	1008.18 (-0.19)	1012.42 (1.87)	1005.75 (-0.05)	1009.38 (0.32)
	NMBF	$-2.0x10^{-4}$	1.8x10-3	-0.034	$3.0x10^{-4}$
	Correlation*	0.94	0.95	0.73	0.93
Wind speed	Observed mean (m s^{-1})	8.09 (n=673)	2.37 (n=620)	6.73 (n=673)	6.0 (n=728)
	Modelled mean (and bias, m s^{-1})	8.19 (0.10)	5.93 (3.55)	6.51 (-0.22)	6.51 (0.51)
	NMBF	0.012	1.50	-0.034	0.085
	Correlation*	0.79	0.67	0.73	0.84
Wind direction	Observed mean (degrees)	143.35 (n=673)	136.89 (n=620)	142.1 (n=673)	137.44 (n=729)
	Modelled mean (and bias, degrees)	127.73 (-15.62)	122.70 (-14.19)	137.84 (-4.26)	118.34 (-19.11)

*All correlation coefficients are statistically significant at $p<0.001$.

Acknowledgements

The ACCESS-EMS-GBR model was set up for the Reef Restoration and Adaptation Program (RRAP) Cooling and Shading Sub-program (RRAP-CS), which is funded by the partnership between the Australian Government Reef Trust and the Great

https://doi.org/10.5194/egusphere-2026-2761
Preprint. Discussion started: 16 July 2026

Barrier Reef Foundation. We would like to acknowledge the RRAP partners: the Australian Institute of Marine Science, the Great Barrier Reef Foundation, Southern Cross University, the University of Queensland, Queensland University of Technology, James Cook University and the CSIRO.

The authors and RRAP partners acknowledge the Traditional Owners of the Great Barrier Reef, as the first reef scientists and carers of Country, and for permission to undertake field measurements on their Sea Country. We specifically acknowledge the Wulgurukaba and Bindal people of the Townsville region, the Warrgamay people of the Lucinda region and the Gooreng Gooreng, Gurang, Bailai and Taribelang Bunda people of the Gladstone to Bundaberg regions for their consent for RRAP-CS to collect atmospheric measurements on their Sea Country.

We thank Professor Hamish Gordon (Carnegie Mellon University) for their work in enabling GLOMAP-mode in the regional UM. We thank Professor Paul Field (University of Leeds, UK Met Office) and Dr Adrian Lock (UK Met Office) for making available their code changes to enable the coupled GLOMAP-CASIM configuration in the regional UM, and Dr Andy Jones (University of Exeter) for their code changes required to implement the updated Abdul-Razzak and Ghan activation scheme.

This research was undertaken with the assistance of resources from the National Computational Infrastructure (NCI Australia), a National Collaborative Research Infrastructure Strategy (NCRIS) enabled capability supported by the Australian Government.

The BRAN2020 reanalysis product, used to produce daily mean sea surface temperature ancillary data, is supported by the Bluelink Partnership: a collaboration between the Australian Department of Defence, the Bureau of Meteorology and CSIRO.

The AERONET AOD measurements were sourced from Australia's Integrated Marine Observing System (IMOS). IMOS, NCRIS and CSIRO are acknowledged for funding the Lucinda Jetty Coastal Observatory. We also thank Dr Thomas Schroeder, CSIRO, for their effort in maintaining the AERONET Lucinda site.

AIMS are acknowledged for the provision of meteorological and seawater measurements in the GBR. The Northern Australia Automated Marine Weather and Oceanographic Station network is part of IMOS and is operated by a consortium of institutions as a joint venture, led by the University of Tasmania.

Financial support

RJ, MW, MB, CL, MM, LH, JH, JA, LC, ZR and DH are funded by RRAP-CS.

ACJ is funded by the Met Office Weather and Climate Science for Service Partnership (WCSSP) India project under the International Science Partnerships Fund (ISPF).

https://doi.org/10.5194/egusphere-2026-2761
Preprint. Discussion started: 16 July 2026

Code availability

Obtaining the UM and UKCA code:

The Unified Model (UM) and United Kingdom Chemistry and Aerosol (UKCA) code and documentation are available under a closed license agreement from the UK Met Office Science Repository Service (https://code.metoffice.gov.uk/). A number of research organisations and national meteorological services use the UM and UKCA in collaboration with the Met Office to undertake research, produce forecasts, develop the code and build and evaluate models. Information on how to apply for a license can be provided by contacting scientific_partnerships@metoffice.gov.uk. Further information is available from the UM (https://www.metoffice.gov.uk/research/approach/modelling-systems/unified-model, last access: 27 May 2026) and UKCA (https://www.metoffice.gov.uk/research/approach/collaboration/jwcrp/ukca, last access: 27 May 2026) Met Office webpages.

Obtaining Rose and Cylc:

The UM is compiled and run from suites, using the Rose suite engine (available from https://github.com/metomi/rose, last access: 27 May 2026) (Shin et al., 2025) and Cylc workflow scheduler (available from https://cylc.github.io/, last access: 27 May 2026) (Oliver et al., 2019). Further information on Rose Cylc configurations are available at https://cylc.github.io/cylc-doc/stable/html/plugins/cylc-rose.html (last access: 27 May 2026). Both Rose and Cylc are available under a GNU General Public License.

Obtaining the ACCESS-EMS-GBR v1.0 model configuration:

The ACCESS-EMS-GBR v1.0 model suite configuration is available to any licensed user of the UM via the Met Office Science Repository Service at https://code.metoffice.gov.uk/trac/roses-u/. The suites have the identifier 'u-ds142' (control aerosol setup, at revision 353745) and 'u-dn070' (revised aerosol setup, at revision 353734). The ancillary files required to run the nested atmospheric domains were generated by the Regional Ancillary Suite with identifier 'u-dr306' (at revision 326287).

Additional code branches required to enable sea salt emissions into the soluble Aitken mode are available from the UM and UKCA repositories (um.xm/branches/dev/matthewwoodhouse/vn13.0_SSinAit and ukca.xm/branches/dev/matthewwoodhouse/um13.0_SSinAit), with additional branches to enable the diagnostic output of primary sea salt emissions to the soluble Aitken mode (um.xm/branches/dev/rebeccajackson/um13.0_AitSSflux and

https://doi.org/10.5194/egusphere-2026-2761
Preprint. Discussion started: 16 July 2026

ukca.xm/branches/dev/rebeccajackson /um13.0_AitSSflux). The revised primary marine organic emission assumptions are implemented in ukca.xm/branches/dev/matthewwoodhouse /um13.0_PMOC_size.

The modified Abdul-Razzak and Ghan (2000) activation scheme, as per the recommendations of Ghosh et al. (2025), is implemented in a UKCA branch for UM v13.0, derived from Andy Jones' revisions for a later version of the model (ukca.xm/branches/dev/rebeccajackson /um13.0_Ghosh_2025, derived from ukca.xm/branches/dev/andyjones/um13.8_ARG2024).

For this paper, ACCESS-EMS-GBR was run and the output stored on NCI. A User Guide for running the ACCESS-EMS-GBR model at NCI is provided in the Supplementary Material.

Obtaining the EMS code:

The EMS model code and documentation are available from the EMS webpage: https://research.csiro.au/cem/software/ems/ (last access: 27 May 2026). A permanent link to the EMS code used in ACCESS-EMS-GBR v1.0 is available under release 1.5.3 (https://github.com/csiro-coasts/EMS/releases/tag/v1.5.3, last access: 27 May 2026) (CSIRO, 2024) and also from the CSIRO Data Portal (https://doi.org/10.25919/a34v-3d81; CSIRO, 2021). Further information on the GBR4 configuration is available on the eReefs project webpage (https://research.csiro.au/ereefs/models/, last access: 27 May 2026).

Analysis:

The analysis scripts used to compare the modelled and observed variables, as well as a script with example model outputs and visualisations are available at https://github.com/rebeccajackson1/access-ems-gbr (last accessed: 27 May 2026).

Data availability

The RRAP-CS field campaign datasets are not currently publicly available but may be provided upon request. The eReefs GBR4 hydrodynamic and biogeochemical hindcast outputs used to initialise the ocean model are available on NCI to users registered to project 'ih54: Coastal Numerical Modelling Collaboration Hub'. The BRAN2020 reanalysis products are available on NCI under project 'gb6: Bluelink Ocean Reanalysis Data Collection'. The AERONET Lucinda AOD data are available from https://aeronet.gsfc.nasa.gov. The AIMS Weather Station and Mooring datasets, and EcoRRAP seawater datasets, are available from https://aims.gov.au/data.

https://doi.org/10.5194/egusphere-2026-2761
Preprint. Discussion started: 16 July 2026

Author contributions

RJ, MW, MB, CL and MM set up the model and coupling framework, with key atmospheric model updates from AJ and DP. DH, MB, MW and RH conceived the study. DH, ZR, LH, JH, JA and LC were involved in the field measurements and data processing. RJ completed the model simulations, data analysis and wrote the manuscript, with revisions from all co-authors.

Competing interests

The authors declare that they have no conflict of interest.

References

Abdul-Razzak, H., & Ghan, S. J. (2000). A parameterization of aerosol activation: 2. Multiple aerosol types. *Journal of Geophysical Research: Atmospheres*, *105*(D5), 6837-6844. https://doi.org/10.1029/1999JD901161

Australian Institute of Marine Science. (2020). *Northern Australia Automated Marine Weather and Oceanographic Stations, Sites: Davies Reef and Heron Island*. https://doi.org/https://doi.org/10.25845/5c09bf93f315d

Baird, M. E., Mongin, M., Rizwi, F., Bay, L. K., Cantin, N. E., Soja-Woźniak, M., & Skerratt, J. (2018). A mechanistic model of coral bleaching due to temperature-mediated light-driven reactive oxygen build-up in zooxanthellae. *Ecological Modelling*, *386*, 20-37. https://doi.org/10.1016/j.ecolmodel.2018.07.013

Baird, M. E., Wild-Allen, K. A., Parslow, J., Mongin, M., Robson, B., Skerratt, J., Rizwi, F., Soja-Woźniak, M., Jones, E., & Herzfeld, M. (2020). CSIRO Environmental Modelling Suite (EMS): Scientific description of the optical and biogeochemical models (vB3p0). *Geoscientific Model Development*, *13*(9), 4503-4553. https://doi.org/10.5194/gmd-13-4503-2020

Best, M. J., Pryor, M., Clark, D., Rooney, G. G., Essery, R., Ménard, C., Edwards, J., Hendry, M., Porson, A., & Gedney, N. (2011). The Joint UK Land Environment Simulator (JULES), model description–Part 1: Energy and water fluxes. *Geoscientific Model Development*, *4*(3), 677-699. https://doi.org/10.5194/gmd-4-677-2011

Buckee, J., Pattiaratchi, C., & Verduin, J. (2020). Partial mortality of intertidal corals due to seasonal daytime low water levels at the Houtman Abrolhos Islands. *Coral Reefs*, *39*, 537-543. https://doi.org/10.1007/s00338-019-01887-5

Bush, M., Allen, T., Bain, C., Boutle, I., Edwards, J., Finnenkoetter, A., Franklin, C., Hanley, K., Lean, H., & Lock, A. (2020). The first Met Office unified model–JULES regional atmosphere and land configuration, RAL1. *Geoscientific Model Development*, *13*(4), 1999-2029. https://doi.org/10.5194/gmd-13-1999-2020

Bush, M., Flack, D. L., Lewis, H. W., Bohnenstengel, S. I., Short, C. J., Franklin, C., Lock, A. P., Best, M., Field, P., & McCabe, A. (2025). The third Met Office Unified Model-JULES Regional Atmosphere and Land Configuration, RAL3. *Geoscientific Model Development*, *18*(12), 3819-3855. https://doi.org/10.5194/gmd-18-3819-2025

https://doi.org/10.5194/egusphere-2026-2761
Preprint. Discussion started: 16 July 2026

Chamberlain, M., Oke, P., Fiedler, R., Beggs, H., Brassington, G., & Divakaran, P. (2021). Next generation of Bluelink ocean reanalysis with multiscale data assimilation: BRAN2020. *Earth System Science Data*, *13*(2). https://doi.org/10.5194/essd-13-5663-2021

Chen, L., Li, Q., Wu, D., Sun, H., Wei, Y., Ding, X., Chen, H., Cheng, T., & Chen, J. (2019). Size distribution and chemical composition of primary particles emitted during open biomass burning processes: Impacts on cloud condensation nuclei activation. *Science of The Total Environment*, *674*, 179-188. https://doi.org/10.1016/j.scitotenv.2019.03.419

Chen, Z., Schofield, R., Rayner, P., Zhang, T., Liu, C., Vincent, C., Fiddes, S., Ryan, R. G., Alroe, J., & Ristovski, Z. D. (2019). Characterization of aerosols over the Great Barrier Reef: The influence of transported continental sources. *Science of The Total Environment*, *690*, 426-437. https://doi.org/10.1016/j.scitotenv.2019.07.007

Cheung, M. W., Hock, K., Skirving, W., & Mumby, P. J. (2021). Cumulative bleaching undermines systemic resilience of the Great Barrier Reef. *Current Biology*, *31*(23), 5385-5392. https://doi.org/10.1016/j.cub.2021.09.078

Clark, D., Mercado, L., Sitch, S., Jones, C., Gedney, N., Best, M., Pryor, M., Rooney, G., Essery, R., & Blyth, E. (2011). The Joint UK Land Environment Simulator (JULES), model description–Part 2: Carbon fluxes and vegetation dynamics. *Geoscientific Model Development*, *4*(3), 701-722. https://doi.org/10.5194/gmd-4-701-2011

CSIRO (2021): EMS Release v1.4.0, https://doi.org/10.25919/a34v-3d81

CSIRO (2024): EMS Release v1.5.3, https://github.com/csiro-coasts/EMS/releases/tag/v1.5.3, last access: 27 May 2026.

Condie, S. A. (2022). Changing the climate risk trajectory for coral reefs. *Frontiers in Climate*, *4*, 980035. https://doi.org/10.3389/fclim.2022.980035

Crippa, M., Guizzardi, D., Pagani, F., Banja, M., Muntean, M., Schaaf, E., Monforti-Ferrario, F., Becker, W. E., Quadrelli, R., Risquez Martin, A., Taghavi-Moharamli, P., Köykkä, J., Grassi, G., Rossi, S., Melo, J., Oom, D., Branco, A., San-Miguel, J., Manca, G., . . . Pekar, F. (2024). *GHG emissions of all world countries.* Publications Office of the European Union. https://data.europa.eu/doi /10.2760/4002897

De'ath, G., Lough, J. M., & Fabricius, K. E. (2009). Declining coral calcification on the Great Barrier Reef. *Science*, *323*(5910), 116-119. https://doi.org/10.1126/science.1165283

Deschaseaux, E. S. M., Swan, H. B., Maher, D., Jones, G. B., Schulz, K., Koveke, E., Toda, K., & Eyre, B. D. (2022). The interplay between dimethyl sulfide (DMS) and methane (CH_4) in a coral reef ecosystem. *Frontiers in Marine Science*, *9*, 910441. https://doi.org/10.3389/fmars.2022.910441

Deschaseaux, E. S. M., Dunne, E., Schulz, K. G., Eyre, B. D., & Harrison, D. P. (2025). The central Great Barrier Reef as a net source of climatically relevant biogenic volatile organic compounds. *Journal of Geophysical Research: Oceans*, *130*(1), e2024JC021192. https://doi.org/10.1029/2024JC021192

Di, Y., Cheung, C. S., & Huang, Z. (2010). Experimental investigation of particulate emissions from a diesel engine fueled with ultralow-sulfur diesel fuel blended with diglyme. *Atmospheric Environment*, *44*(1), 55-63. https://doi.org/10.1016/j.atmosenv.2009.09.039

https://doi.org/10.5194/egusphere-2026-2761
Preprint. Discussion started: 16 July 2026

Duncan, E. K., Jordan, G., Kim, P., Haywood, J., Watson-Parris, D., Johnson, B., Sellar, A., Kipling, Z., Teixeira, J., Malavelle, F., & Partridge, D. (2026). Lagrangian investigation of GCMs during the 2014-15 Holuhraun eruption reveals large differences in the representation of aerosol size distribution. *Atmospheric Chemistry and Physics Discussions*. https://doi.org/10.5194/egusphere-2026-1043

Eckert, C., Hernandez-Jaramillo, D. C., Medcraft, C., Harrison, D. P., & Kelaher, B. P. (2024). Drone-Based Measurement of the Size Distribution and Concentration of Marine Aerosols above the Great Barrier Reef. *Drones*, *8*(7), 292.

Edwards, J. M., & Slingo, A. (1996). Studies with a flexible new radiation code. I: Choosing a configuration for a large-scale model. *Quarterly Journal of the Royal Meteorological Society*, *122*, 689-719. https://doi.org/10.1002/qj.49712253107

Egbert, G. D., & Erofeeva, S. Y. (2002). Efficient inverse modeling of barotropic ocean tides. *Journal of Atmospheric and Oceanic technology*, *19*(2), 183-204. https://doi.org/10.1175/1520-0426(2002)019<0183:EIMOBO>2.0.CO;2

Ellis, R. (2018). Dynamic SedNet component model reference guide: Update 2017, Concepts and algorithms used in Source Catchments customisation plugin for Great Barrier Reef catchment modelling. Queensland Department of Environment and Science, Bundaberg, Queensland. 38 pp.

Ellis, S. L., Baird, M. E., Harrison, L. P., Schulz, K. G., & Harrison, D. P. (2025). A photophysiological model of coral bleaching under light and temperature stress: experimental assessment. *Conservation Physiology*, *13*(1), coaf020. https://doi.org/10.1093/conphys/coaf020

Emmerson, K. M., Galbally, I. E., Guenther, A. B., Paton-Walsh, C., Guerette, E.-A., Cope, M. E., Keywood, M. D., Lawson, S. J., Molloy, S. B., & Dunne, E. (2016). Current estimates of biogenic emissions from eucalypts uncertain for southeast Australia. *Atmospheric Chemistry and Physics*, *16*(11), 6997-7011. https://doi.org/10.5194/acp-16-6997-2016

Fiddes, S. L., Woodhouse, M. T., Mallet, M. D., Lamprey, L. J., Humphries, R. S., Protat, A., Alexander, S. P., Hayashida, H., Putland, S., & Miljevic, B. (2025). The ACCESS-AM2 climate model underestimates aerosol concentration in the Southern Ocean; improving aerosol representation could be problematic for the global energy balance. *Atmospheric Chemistry and Physics*, *25*(22), 16451-16477. https://doi.org/10.5194/acp-25-16451-2025

Fiddes, S. L., Woodhouse, M. T., Utembe, S., Schofield, R., Alexander, S. P., Alroe, J., Chambers, S. D., Chen, Z., Cravigan, L., & Dunne, E. (2022). The contribution of coral-reef-derived dimethyl sulfide to aerosol burden over the Great Barrier Reef: a modelling study. *Atmospheric Chemistry and Physics*, *22*, 2419-2445. https://doi.org/10.5194/acp-22-2419-2022

Field, P. R., Hill, A., Shipway, B., Furtado, K., Wilkinson, J., Miltenberger, A., Gordon, H., Grosvenor, D. P., Stevens, R., & Van Weverberg, K. (2023). Implementation of a double moment cloud microphysics scheme in the UK Met Office regional numerical weather prediction model. *Quarterly Journal of the Royal Meteorological Society*, *149*(752), 703-739. https://doi.org/10.1002/qj.4414

Gantt, B., Johnson, M., Meskhidze, N., Sciare, J., Ovadnevaite, J., Ceburnis, D., & O'Dowd, C. (2012). Model evaluation of marine primary organic aerosol emission schemes. *Atmospheric Chemistry and Physics*, *12*(18), 8553-8566. https://doi.org/10.5194/acp-12-8553-2012

https://doi.org/10.5194/egusphere-2026-2761
Preprint. Discussion started: 16 July 2026

Gantt, B., Johnson, M. S., Crippa, M., Prévôt, A. S., & Meskhidze, N. (2015). Implementing marine organic aerosols into the GEOS-Chem model. *Geoscientific Model Development*, *8*(3), 619-629. https://doi.org/10.5194/gmd-8-619-2015

Gillibrand, P., & Herzfeld, M. (2016). A mass-conserving advection scheme for offline simulation of scalar transport in coastal ocean models. *Ocean Modelling*, *101*, 1-16. https://doi.org/10.1016/j.ocemod.2016.02.008

Giorgi, F. (2019). Thirty years of regional climate modeling: where are we and where are we going next? *Journal of Geophysical Research: Atmospheres*, *124*(11), 5696-5723.

Gong, S. (2003). A parameterization of sea-salt aerosol source function for sub-and super-micron particles. *Global Biogeochemical Cycles*, *17*(4). https://doi.org/10.1029/2003GB002079

Grant, W. D., & Madsen, O. S. (1982). Movable bed roughness in unsteady oscillatory flow. *Journal of Geophysical Research: Oceans*, *87*(C1), 469-481. https://doi.org/10.1029/JC087iC01p00469

Harrison, D. P. (2024). An overview of environmental engineering methods for reducing coral bleaching stress. In E. Wolanski & M. J. Kingsford (Eds.), *Oceanographic Processes of Coral Reefs: Physical and Biological Links in the Great Barrier Reef* (pp. 403-418). https://doi.org/https://doi.org/10.1201/9781003320425

Harrison, D. P., Baird, M., Harrison, L., Utembe, S., Schofield, R., Escobar-Correa, R., Mongin, M., & Rizwi, F. (2019). Environmental Modelling of Large Scale Solar Radiation Management. A report provided to the Australian Government by the Reef Restoration and Adaptation Program, Townsville, Australia. 83 pp.

He, X. C., Abraham, N. L., Ding, H., Russo, M. R., Grosvenor, D. P., Ge, Y., Wang, X., Jones, A. C., Campuzano-Jost, P., & Nault, B. (2026). Evaluation of UKESM aerosol size and composition using Atom measurements indicates missing marine aerosol formation mechanisms. *Atmospheric Chemistry and Physics*, *26*(5), 3805-3851. https:/doi.org/10.5194/acp-26-3805-2026

Hersbach, H., Bell, B., Berrisford, P., Hirahara, S., Horányi, A., Muñoz-Sabater, J., Nicolas, J., Peubey, C., Radu, R., & Schepers, D. (2020). The ERA5 global reanalysis. *Quarterly Journal of the Royal Meteorological Society*, *146*, 1999-2049. https://doi.org/10.1002/qj.3803

Herzfeld, M. (2006). An alternative coordinate system for solving finite difference ocean models. *Ocean Modelling*, *14*(3-4), 174-196. https://doi.org/10.1016/j.ocemod.2006.04.002

Herzfeld, M., & Engwirda, D. (2023). A Flux-Form Semi-Lagrangian advection scheme for tracer transport on arbitrary meshes. *Ocean Modelling*, *181*, 102140. https://doi.org/10.1016/j.ocemod.2022.102140

Hopkins, F. E., Bell, T. G., Yang, M., Suggett, D. J., & Steinke, M. (2016). Air exposure of coral is a significant source of dimethylsulfide (DMS) to the atmosphere. *Scientific Reports*, *6*, 1-11. https://doi.org/10.1038/srep36031

Horchler, E. J., Alroe, J., Harrison, L., Cravigan, L., Harrison, D. P., & Ristovski, Z. D. (2025). Measurement report: Aerosol and cloud nuclei properties along the Central and Northern Great Barrier Reef–impact of continental emissions. *Atmospheric Chemistry and Physics*, *25*(17), 10075-10087. https://doi.org/10.5194/acp-25-10075-2025

https://doi.org/10.5194/egusphere-2026-2761
Preprint. Discussion started: 16 July 2026

Hughes, T. P., Kerry, J. T., Baird, A. H., Connolly, S. R., Chase, T. J., Dietzel, A., Hill, T., Hoey, A. S., Hoogenboom, M. O., & Jacobson, M. (2019). Global warming impairs stock–recruitment dynamics of corals. *Nature*, *568*, 387-390. https://doi.org/10.1038/s41586-019-1081-y

Hughes, T. P., Kerry, J. T., Connolly, S. R., Álvarez-Romero, J. G., Eakin, C. M., Heron, S. F., Gonzalez, M. A., & Moneghetti, J. (2021). Emergent properties in the responses of tropical corals to recurrent climate extremes. *Current Biology*, *31*(23), 5393-5399. e5393. https://doi.org/10.1016/j.cub.2021.10.046

International Maritime Organisation (IMO), *MARPOL Annex VI – Regulations for the Prevention of Air Pollution from Ships*, Regulation 14 (Sulphur Oxides), 2020.IPCC. (2023). Climate Change 2023: Synthesis Report. Contribution of Working Groups I, II and III to the Sixth Assessment Report of the Intergovernmental Panel on Climate Change. In [Core Writing Team, H. Lee, & J. Romero (eds.)]. Geneva, Switzerland. 184 pp. https://10.59327/IPCC/AR6-9789291691647

Jackson, R. L., Gabric, A. J., Cropp, R. A., & Woodhouse, M. T. (2020). Dimethylsulfide (DMS), marine biogenic aerosols and the ecophysiology of coral reefs. *Biogeosciences*, *17*(8), 2181-2204. https://doi.org/10.5194/bg-17-2181-2020

Jackson, R. L., Woodhouse, M. T., & Harrison, D. P. (*in prep*). Optimising sea spray aerosol emissions for marine sky and cloud brightening over the Great Barrier Reef, Australia. *Atmospheric Chemistry and Physics*.

Kiss, A. E., Hogg, A. M., Hannah, N., Boeira Dias, F., Brassington, G. B., Chamberlain, M. A., Chapman, C., Dobrohotoff, P., Domingues, C. M., & Duran, E. R. (2020). ACCESS-OM2 v1.0: A global ocean–sea ice model at three resolutions. *Geoscientific Model Development*, *13*(2), 401-442. https://doi.org/10.5194/gmd-13-401-2020

Kleypas, J., Allemand, D., Anthony, K., Baker, A. C., Beck, M. W., Hale, L. Z., Hilmi, N., Hoegh-Guldberg, O., Hughes, T., & Kaufman, L. (2021). Designing a blueprint for coral reef survival. *Biological Conservation*, *257*, 109107. https://doi.org/10.1016/j.biocon.2021.109107

Kwiatkowski, L., Cox, P., Halloran, P. R., Mumby, P. J., & Wiltshire, A. J. (2015). Coral bleaching under unconventional scenarios of climate warming and ocean acidification. *Nature Climate Change*, *5*, 777-781. https://doi.org/10.1038/nclimate2655

Latham, J. (1990). Control of global warming? *Nature*, *347*, 339-340. https://doi.org/10.1038/347339b0

Latham, J. (2004). Amelioration of global warming by controlled enhancements of the albedo and longevity of low-level marine clouds. *Atmospheric Science Letters*, *3*, 52-58. https://dio.org/10.1006/asle.2002.0099

Lesser, M. P. (2011). Coral bleaching: causes and mechanisms. In Z. Dubinsky & N. Stambler (Eds.), *Coral Reefs: An Ecosystem in Transition* (pp. 405-419). Springer, Dordrecht. https://doi.org/https://doi.org/10.1007/978-94-007-0114-4_23

Liu, G., Strong, A. E., Skirving, W., & Arzayus, L. F. (2006). Overview of NOAA coral reef watch program's near-real time satellite global coral bleaching monitoring activities. *Proceedings of the 10th International Coral Reef Symposium*, *1793*, 1783-1793. https://www.researchgate.net/publication/284342045

Madsen, O. S. (1994). Spectral wave-current bottom boundary layer flows. In *Coastal Engineering 1994* (pp. 384-398). https://doi.org/https://doi.org/10.1061/9780784400890.030

Maggiorano, A., Baird, M., Langlais, C., Mongin, M., & Skerratt, J. (2025). Impact of phytoplankton, CDOM, and suspended sediments on the vertical attenuation of light, changing heat content and circulation on a continental shelf: a modelling study of the Great Barrier Reef. *Ocean Modelling*, *193*, 102465. https://doi.org/10.1016/j.ocemod.2024.102465

Mallet, M., Cravigan, L., Miljevic, B., Vaattovaara, P., Deschaseaux, E. S. M., Swan, H. B., Jones, G., & Ristovski, Z. (2016). Sea spray aerosol in the Great Barrier Reef and the prescence of nonvolatile organics. *Journal of Geophysical Research: Atmospheres*, *121*(12), 7088-7099. https://doi.org/10.1002/2016JD024966

Mann, G. W., Carslaw, K. S., Ridley, D. A., Spracklen, D. V., Pringle, K. J., Merikanto, J., Korhonen, H., Schwarz, J. P., Lee, L. A., & Manktelow, P. T. (2012). Intercomparison of modal and sectional aerosol microphysics representations within the same 3-D global chemical transport model. *Atmospheric Chemistry and Physics*, *12*, 4449-4476. https://doi.org/10.5194/acp-12-4449-2012

Mann, G. W., Carslaw, K. S., Spracklen, D. V., Ridley, D. A., Manktelow, P. T., Chipperfield, M. P., Pickering, S. J., & Johnson, C. E. (2010). Description and evaluation of GLOMAP-mode: A modal global aerosol microphysics model for the UKCA composition-climate model. *Geoscientific Model Development*, *3*, 519-551. https://doi.org/10.5194/gmd-3-519-2010

Margvelashvili, N. (2009). Stretched Eulerian coordinate model of coastal sediment transport. *Computers & Geosciences*, *35*(6), 1167-1176. https://doi.org/10.1016/j.cageo.2008.03.016

Margvelashvili, N., Andrewartha, J., Baird, M., Herzfeld, M., Jones, E., Mongin, M., Rizwi, F., Robson, B., Skerratt, J., & Wild-Allen, K. (2018). Simulated fate of catchment-derived sediment on the Great Barrier Reef shelf. *Marine Pollution Bulletin*, *135*, 954-962. https://doi.org/10.1016/j.marpolbul.2018.08.018

McCloskey, G., Baheerathan, R., Dougall, C., Ellis, R., Bennett, F., Waters, D., Darr, S., Fentie, B., Hateley, L., & Askildsen, M. (2021). Modelled estimates of fine sediment and particulate nutrients delivered from the Great Barrier Reef catchments. *Marine Pollution Bulletin*, *165*, 112163. https://doi.org/10.1016/j.marpolbul.2021.112163

McDonald, J., McGee, J., Brent, K., & Burns, W. (2019). Governing geoengineering research for the Great Barrier Reef. *Climate Policy*, *19*(7), 801-811. https://doi.org/10.1080/14693062.2019.1592742

McGowan, H., Lensky, N. G., Abir, S., & Saunders, M. (2022). Coral Reef Coupling to the Atmospheric Boundary Layer Through Exchanges of Heat, Moisture, and Momentum: Case Studies From Tropical and Desert Fringing Coral Reefs. *Frontiers in Marine Science*, 983. https://doi.org/10.3389/fmars.2022.900679

Melbourne-Thomas, J., Johnson, C. R., Fung, T., Seymour, R. M., Chérubin, L. M., Arias-González, J. E., & Fulton, E. A. (2011). Regional-scale scenario modeling for coral reefs: a decision support tool to inform management of a complex system. *Ecological Applications*, *21*(4), 1380-1398. https://doi.org/10.1890/09-1564.1

Metzger, A., Verheggen, B., Dommen, J., Duplissy, J., Prevot, A. S., Weingartner, E., Riipinen, I., Kulmala, M., Spracklen, D. V., & Carslaw, K. S. (2010). Evidence for the role of organics in aerosol particle formation under atmospheric conditions. *Proceedings of the National Academy of Sciences*, *107*(15), 6646-6651. https://doi.org/10.1073/pnas.0911330107

https://doi.org/10.5194/egusphere-2026-2761
Preprint. Discussion started: 16 July 2026

Oliver, H., Shin, M., Matthews, D., Sanders, O., Bartholomew, S., Clark, A., Fitzpatrick, B., van Haren, R., Hut, R., & Drost, N. (2019). Workflow automation for cycling systems. *Computing in Science and Engineering*, *21*(4), 7-21. https://doi.org/10.1109/MCSE.2019.2906593

Pokhrel, R. P., Gordon, J., Fiddler, M. N., & Bililign, S. (2021). Impact of combustion conditions on physical and morphological properties of biomass burning aerosol. *Aerosol Science and Technology*, *55*(1), 80-91. https://doi.org/10.1080/02786826.2020.1822512

Pratchett, M. S., Heron, S. F., Mellin, C., & Cumming, G. S. (2021). Recurrent mass-bleaching and the potential for ecosystem collapse on Australia's Great Barrier Reef. In *Ecosystem collapse and climate change* (pp. 265-289). Springer, https://doi.org/https://doi.org/10.1007/978-3-030-71330-0_10

Ranjithkumar, A., Gordon, H., Williamson, C., Rollins, A., Pringle, K., Kupc, A, Abraham, N. L., Brock, C., & Carslaw, K. (2021). Constraints on global aerosol number concentration, SO_2 and condensation sink in UKESM1 using Atom measurements. *Atmospheric Chemistry and Physics*, *21*, 4979-5014. https://doi.org/10.5194/acp-21-4979-2021

Rayner, N., Parker, D., Horton, E., Folland, C. K., Alexander, L. V., Rowell, D., Kent, E. C., & Kaplan, A. (2003). Global analyses of sea surface temperature, sea ice, and night marine air temperature since the late nineteenth century. *Journal of Geophysical Research: Atmospheres*, *108*(D14). https://doi.org/10.1029/2002JD002670

Razak, T. B., Roff, G., Lough, J. M., & Mumby, P. J. (2020). Growth responses of branching versus massive corals to ocean warming on the Great Barrier Reef, Australia. *Science of The Total Environment*, *705*, 135908. https://doi.org/10.1016/j.scitotenv.2019.135908

Richards, L. S., Siems, S. T., Huang, Y., Zhao, W., Harrison, D. P., Manton, M. J., & Reeder, M. J. (2024). The meteorological drivers of mass coral bleaching on the central Great Barrier Reef during the 2022 La Nina. *Scientific Reports*, *14*, 23867. https://doi.org/10.1038/s41598-024-74181-2

Richards, L. S., Siems, S. T., Huang, Y., Harrison, D. P., & Zhao, W. (2026). Trade wind regimes during the Great Barrier Reef coral bleaching season. *Weather and Climate Regimes*, *7*, 109-127. https://doi.org/10.5194/wcd-7-109-2026

Reid, J., Koppmann, R., Eck, T., & Eleuterio, D. (2005). A review of biomass burning emissions part II: intensive physical properties of biomass burning particles. *Atmospheric Chemistry and Physics*, *5*(3), 799-825. https://doi.org/10.5194/acp-5-799-2005

Shin, M., Fitzpatrick, B., Clark, A., Sanders, O., Pillinger, T., Dutta, R., Bartholomew, S. L., Whitehouse, S., Matthews, D., Oxley, S., Trzeciak, T., Valters, D., Oliver, H. J., Mancell, J., Hall, M., Coleman, T., Shepherd, H., Osprey, A., Seddon, J., Theodorakis, D., Joe, R., Abram, J., Dix, M., Sharp, R., Frost, J., Dawson, M., and Cresswell, P. (2025): metomi/rose: Rose 2.4.2 (2.4.2), Zenodo [code], https://doi.org/10.5281/zenodo.15169210.

Shipway, B. J., & Hill, A. A. (2012). Diagnosis of systematic differences between multiple parametrizations of warm rain microphysics using a kinematic framework. *Quarterly Journal of the Royal Meteorological Society*, *138*(669), 2196-2211. https://doi.org/10.1002/qj.1913

Sindelarova, K., Granier, C., Bouarar, I., Guenther, A., Tilmes, S., Stavrakou, T., Müller, J.-F., Kuhn, U., Stefani, P., & Knorr, W. (2014). Global data set of biogenic VOC emissions calculated by the MEGAN model over the last 30 years. *Atmospheric Chemistry and Physics*, *14*(17), 9317-9341. https://doi.org/10.5194/acp-14-9317-2014

https://doi.org/10.5194/egusphere-2026-2761
Preprint. Discussion started: 16 July 2026

Skerratt, J., Mongin, M., Baird, M., Wild-Allen, K., Robson, B., Schaffelke, B., Davies, C., Richardson, A., Margvelashvili, N., & Soja-Wozniak, M. (2019). Simulated nutrient and plankton dynamics in the Great Barrier Reef (2011–2016). *Journal of Marine Systems*, *192*, 51-74. https://doi.org/10.1016/j.jmarsys.2018.12.006

Steven, A. D., Baird, M. E., Brinkman, R., Car, N. J., Cox, S. J., Herzfeld, M., Hodge, J., Jones, E., King, E., & Margvelashvili, N. (2019). eReefs: An operational information system for managing the Great Barrier Reef. *Journal of Operational Oceanography*, *12*(sup2), S12-S28. https://doi.org/10.1080/1755876X.2019.1650589

Stier, P., Feichter, J., Kinne, S., Kloster, S., Vignati, E., Wilson, J., Ganzeveld, L., Tegen, I., Werner, M., & Balkanski, Y. (2005). The aerosol-climate model ECHAM5-HAM. *Atmospheric Chemistry and Physics*, *5*(4), 1125-1156. https://doi.org/10.5194/acp-5-1125-2005

Suggett, D. J., & Smith, D. J. (2020). Coral bleaching patterns are the outcome of complex biological and environmental networking. *Global Change Biology*, *26*(1), 68-79. https://doi.org/10.1111/gcb.14871

Swan, H. B., Jones, G. B., Deschaseaux, E. S. M., & Eyre, B. D. (2017). Coral reef origins of atmospheric dimethylsulfide at Heron Island, southern Great Barrier Reef, Australia. *Biogeosciences*, *14*, 229-239. https://doi.org/10.5194/bg-14-229-2017

Tagliafico, A., Baker, P., Kelaher, B., Ellis, S., & Harrison, D. (2022). The Effects of Shade and Light on Corals in the Context of Coral Bleaching and Shading Technologies. *Frontiers in Marine Science*, 1150. https://doi.org/10.3389/fmars.2022.919382

Talvinen, S., Kim, P., Tovazzi, E., Holopainen, E., Cremer, R., Kühn, T., Kokkola, H., Kipling, Z., Neubauer, D., & Teixeira, J. C. (2025). Towards an improved understanding of the impact of clouds and precipitation on the representation of aerosols over the Boreal Forest in GCMs. *Atmospheric Chemistry and Physics*, *25*(21), 14449-14478. https://doi.org/10.5194/acp-25-14449-2025

Tippett, A., Field, P. R., & Gryspeerdt, E. (2026). Evaluating simulations of ship tracks in a km-scale model. *Atmospheric Chemistry and Physics*, *26*(6), 4251-4274. https://doi.org/10.5194/acp-26-4251-2026

Tiwari, M., Sahu, S. K., Bhangare, R. C., Yousaf, A., & Pandit, G. G. (2014). Particle size distributions of ultrafine combustion aerosols generated from household fuels. *Atmospheric Pollution Research*, *5*(1), 145-150. https://doi.org/10.5094/APR.2014.018

Twomey, S. (1974). Pollution and the planetary albedo. *Atmospheric Environment (1967)*, *8*, 1251-1256. https://doi.org/10.1016/0004-6981(74)90004-3

Venugopal, A. U., Bhatti, Y. A., Morgenstern, O., Williams, J., Edkins, N., Hardacre, C., Jones, A., & Revell, L. E. (2025). Constraining the uncertainty associated with sea salt aerosol parameterizations in global models using nudged UKESM1-AMIP simulations. *Journal of Geophysical Research: Atmospheres*, *130*(2), e2024JD041643. https://doi.org/10.1029/2024JD041643

Willett, M. R., Brooks, M., Bushell, A., Earnshaw, P., Smith, S., Tomassini, L., Best, M., Boutle, I., Brooke, J., & Edwards, J. M. (2026). The Met Office Unified Model Global Atmosphere 8.0 and JULES Global Land 9.0 configurations. *EGUsphere*, *19*(4), 1473–1517. https://doi.org/10.5194/gmd-19-1473-2026

https://doi.org/10.5194/egusphere-2026-2761
Preprint. Discussion started: 16 July 2026

Wilson, D. R., Bushell, A. C., Kerr-Munslow, A. M., Price, J. D., & Morcrette, C. J. (2008). PC2: A prognostic cloud fraction and condensation scheme. I: Scheme description. *Quarterly Journal of the Royal Meteorological Society: A journal of the atmospheric sciences, applied meteorology and physical oceanography*, *134*(637), 2093-2107. https://doi.org/10.1002/qj.333

Woodward, S. (2001). Modeling the atmospheric life cycle and radiative impact of mineral dust in the Hadley Centre climate model. *Journal of Geophysical Research: Atmospheres*, *106*(D16), 18155-18166. https://doi.org/10.1029/2000JD900795

Yu, S., Eder, B., Dennis, R., Chu, S. H., & Schwartz, S. E. (2006). New unbiased symmetric metrics for evaluation of air quality models. *Atmospheric Science Letters*, *7*(1), 26-34. https://doi.org/10.1002/asl.125

Zhuang, J., Dussin, R., Huar, D., Bourgault, P., Banihirw, A., Raynaud, S., Malevich, B., Schupfner, M., Filipe, Gauthier, C., Levang, S., Jüling, A., Almansi, M., Rasp, S., Smith, T. J., Mares, B., Stachelek, J., Ploug, M., Pierr, . . . Li, X. (2025). *pangeo-data/xESMF: v0.8.10*. In Zenodo.

Zieger, S. (2025). The Australian wave forecast system with statistical wind correction, *Journal of Southern Hemisphere Earth Systems Science*, *75*(2), ES25010, https://doi.org/10.1071/ES25010.

Zieger, S., & Greenslade, D. (2021). A multiple-resolution global wave model – AUSWAVE-G3, *Bureau Research Report No 51*, Bureau of Meteorology, Melbourne, Australia, 74 pp. http://www.bom.gov.au/research/publications/researchreports/BRR-051.pdf.

Zillman, J. W. (1972). A study of some aspects of the radiation and heat budgets of the Southern Hemisphere oceans. In *Meteorological study no. 26*. Canberra, Australia.